Fig. 1. (A) Distribution of anti-UACA IgG autoantibodies titer in healthy controls (control), in patients with Graves' disease (Graves), Hashimoto's disease (Hashimoto), silent thyroiditis (silent), and subacute thyroiditis (subacute). The titers of autoantibodies are expressed in the OD units. Broken line indicates a cutoff level for the positivity of autoantibody. The OD value subtracted GST protein from GST–UACA fusion protein in 159 Graves' disease samples was 0.339 ± 0.305 (mean ± SE), in 26 Hashimoto's thyroiditis samples was 0.269 ± 0.151 (mean ± SE), in 20 silent thyroiditis samples was 0.269 ± 0.156 (mean ± SE), in 11 subacute thyroiditis samples was 0.315 ± 0.130 (mean ± SE), and in 43 healthy control samples was 0.218 ± 0.103 (mean ± SE). The OD value for GST–UACA fusion protein to GST protein in 27 positive samples was 0.865 ± 0.384 (mean ± SE), and in negative samples was 0.240 ± 0.125 (mean ± SE). *Significant difference ($P < 0.01$) compared with control (ANOVA). (B) Distribution of anti-UACA IgG autoantibodies titer in patients with Graves' ophthalmopathy. The clinical manifestations of Graves' ophthalmopathy are classified into the following four groups; normal MRI, congestive ophthalmopathy with severe fat swelling, congestive ophthalmopathy with mild myopathy, and severe myopathy. The OD value subtracted GST protein from GST–UACA fusion protein in seven normal MRI samples was 0.167 ± 0.098 (mean ± SE), in three congestive ophthalmopathy with severe fat swelling samples was 0.255 ± 0.029 (mean ± SE), in seven congestive ophthalmopathy with mild myopathy samples was 0.418 ± 0.395 (mean ± SE), and in eight severe myopathy samples was 0.656 ± 0.349 (mean ± SE). *Significant difference ($P < 0.005$) compared with normal MRI (ANOVA). NS: not significant.

were not statistically significant between Hashimoto's thyroiditis and healthy control, silent thyroiditis and healthy control, and subacute thyroiditis and healthy control. More than half of Graves' patients with positive titer showed higher titer than patients with VKH disease. Positive patient sera with VKH disease showed about 0.5 OD value in the same ELISA.

Clinical manifestation

We investigated clinical manifestation of Graves' patients with high anti-UACA titer in detail. We found 37.5% (9/24) cases had ophthalmopathy. Especially, patient samples with severe eye muscle inflammation showed high anti-UACA titer. Nine cases with Graves'

Table 1
Prevalence of IgG anti-UACA autoantibodies evaluated by ELISA in sera from patients with thyroid diseases and healthy controls

Disease	Anti-human UACA IgG positive donors		P value
Graves' disease	24/159	15%	P < 0.01
Hashimoto's disease	1/26	4%	
Silent thyroiditis	1/20	5%	
Subacute thyroiditis	1/11	9%	
Healthy controls	0/43	0%	

Differences in prevalence of IgG anti-UACA autoantibodies are statistically significant between patients with Graves' disease and healthy controls using Fisher's exact test (2 × 2 table).

Table 3
Prevalence of IgG anti-UACA autoantibodies evaluated by ELISA in sera from patients with Graves' ophthalmopathy and MRI study

Group	Anti-human UACA IgG positive donors		P value
Severe ocular myopathy	6/8	75%	P < 0.01
Congestive ophthalmopathy (with mild myopathy)	2/7	28%	
Congestive ophthalmopathy (with severe orbital fat swelling)	0/3	0%	.
Normal MRI	0/7	0%	

Statistical analyses refer to differences between patients with severe ocular myopathy and Normal MRI group determined using Fisher's exact test (2 × 2 table).

ophthalmopathy showed high titer (OD value >0.53) within 31 Graves' ophthalmopathy cases. The prevalence of anti-UACA antibodies was 29% in Graves' ophthalmopathy cases. But, the prevalence of anti-UACA antibodies in patients without ophthalmopathy was 11% (15/128). The prevalence of Graves' ophthalmopathy cases was significantly higher than that of Graves' patients without ophthalmopathy (Fisher's exact test; P < 0.05) (Table 2). Within nine cases of high titer, six cases showed severe eye muscle inflammation in MRI study. Graves' ophthalmopathy is classified into the following four groups; severe ocular myopathy, congestive ophthalmopathy with mild myopathy, congestive ophthalmopathy with severe orbital fat swelling and without myopathy, and normal MRI. The prevalence of anti-UACA antibodies was 75% (6/8) in severe ocular myopathy, which had severe eye muscle enlargement and high intensity signal within eye muscle in T2WI MRI study. In contrast, the prevalence of anti-UACA antibodies was 28% (2/7) in congestive ophthalmopathy cases with mild myopathy, who had mild eye muscle enlargement and high intensity signal in T2WI MRI study. The prevalence of anti-UACA antibodies was 0% (0/3) in congestive ophthalmopathy case, who had severe orbital fat swelling, no eye muscle enlargement, and no high intensity in T2WI MRI study. UACA titer of seven patients with normal MRI study was all normal.

The mean UACA titer of severe ocular myopathy cases was significantly higher than that of seven normal

Table 2
Prevalence of IgG anti-UACA autoantibodies evaluated by ELISA in sera from patients with Graves' ophthalmopathy and without Graves' ophthalmopathy

Group	Anti-human UACA IgG positive donors		P value
Graves' ophthalmopathy (+)	9/31	29%	P < 0.05
Graves' ophthalmopathy (−)	15/128	11%	

Statistical analyses refer to differences between patients with Graves' ophthalmopathy and without Graves' ophthalmopathy determined using χ^2 test (2 × 2 table, Yeasts' correction for small numbers).

cases in MRI study (ANOVA; P < 0.005) (Fig. 1B). The prevalence of anti-UACA antibodies was 75% (6/8) in patients with severe ocular myopathy. The prevalence was significantly higher than that of normal MRI group (Fisher's exact test; P < 0.01) (Table 3). But, any other group did not show the significant difference compared with normal MRI group.

Expression of UACA in thyroid

To examine mRNA expression of UACA in thyroid, we performed RT-PCR analysis (Fig. 2C). Gene-specific PCR primers were designed to amplify 505 bp fragments of C-terminal portion of human UACA cDNA. The expression of UACA mRNA was observed in all human thyroid cancer cell lines (HTC, 8505C, FRO, and NPA), as well as human thyroid tissue of Graves' disease, Hashimoto's thyroiditis, and normal control. This result indicates UACA mRNA is expressed in human thyroid follicular cells.

To examine the expression profile of UACA protein in FRTL5 cell, we performed Western blot analysis. UACA encoded 160 kDa protein (Figs. 2A and B). The amount of UACA protein was augmented in a time (0, 3, 6, 12, and 24 h) (Fig. 2A) and dose-dependent manner following TSH stimulation (0, 10^{-3}, 10^{-2}, 10^{-1}, and 1 mU/ml) (Fig. 2B). In a time course, UACA protein increased after 3 h following TSH stimulation. The strongest signal was observed after 6 or 12 h following TSH stimulation, and the signal decreased after 24 h following TSH stimulation. In a dose course of TSH, the minimum concentration of TSH to increase UACA protein was 10^{-3} mU/ml.

In order to study the cytochemical localization of UACA, we estimated the expression of UACA in FRTL5 cells. The UACA protein was weakly expressed both in nucleus and cytoplasm of cells in the absence of TSH (Fig. 3A). Interestingly, TSH stimulation recruited UACA into nucleus (Fig. 3A; 24 h). In order to observe the fine localization of UACA within TSH-stimulated
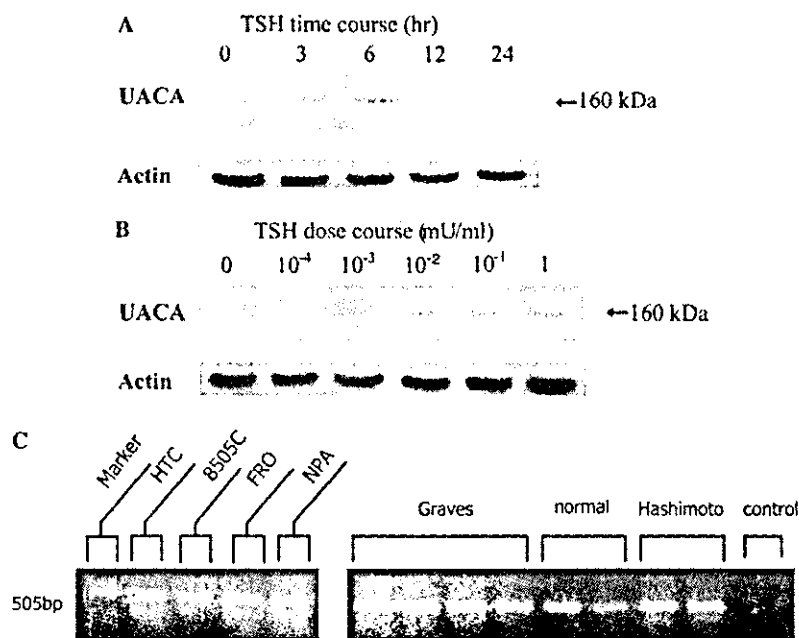
Fig. 2. TSH potentiates UACA protein expression in FRTL5 thyroid cells: (A) time sequence, (B) dose dependency. FRTL5 cells were preincubated in 5H medium with 5% CS for 5–6 days and then incubated with appropriate concentrations of TSH. To ensure the total amount of protein in each lane was identical, membranes were simultaneously incubated with anti-actin antibody (1:250 dilution). (C) RT-PCR analysis using human UACA-specific primers revealed the expression of UACA mRNA in human thyroid cancer cell lines (HTC, 8505C, FRO, and NPA), and the thyroid tissue of Grave's disease, Hashimoto's disease, and normal subject. Control lane indicates PCR product when any template was not included in PCR.

FRTL5, we used a differential interference contrast image. Most of the UACA fluorescence was localized within nucleus, whereas less was localized in cytoplasm (Fig. 3B). To examine UACA expression in human thyroid tissue, we then carried out an immunohistochemical analysis using rabbit polyclonal anti-UACA antibody. In thyroid tissue of Graves' disease, UACA appeared to be expressed in the nucleus of thyroid follicular cells (Fig. 3C).

Expression of UACA protein in eye muscle

In order to investigate the association of Graves' ophthalmopathy and anti-UACA antibody production, we examined UACA expression in human eye muscle derived from a patient with Graves' ophthalmopathy. In human eye muscle tissue with Graves' ophthalmopathy, UACA protein was exclusively expressed in eye muscle fiber (arrow), but UACA expression was relatively weak in surrounding orbital connective tissue and fat (Fig. 3D). The eye muscle sample was derived from a patient with Graves' ophthalmopathy, who was already treated by methimazole and corticosteroid. Since this pretreatment may modify the UACA expression in eye muscle, we simultaneously examined UACA expression in normal rat eye muscle. UACA protein was expressed in normal rat eye muscle fiber as observed in the human sample (data not shown). This result indicates UACA

is expressed in eye muscle fiber as well as thyroid cells, which are the autoimmune target tissues in Graves' disease.

Discussion

UACA is a protein cloned by serological analysis of recombinant cDNA expression libraries (SEREX) method with serum samples obtained from patients with VKH disease, to identify the target autoantigens in VKH disease [1]. VKH disease is recognized as an autoimmune systemic disorder. In VKH, inflammatory disorders in multiple organs include melanocytes, uvea (resulting in acute bilateral panuveitis), skin (vitiligo and alopecia), central nervous system (meningitis), and inner ears (hearing loss and tinnitus). These inflammatory aspects are attributed to the immunological destruction of melanocytes. The prevalence of IgG anti-UACA autoantibodies is 19.6% in patients with VKH, and 0% in the healthy controls, 28.1% in patients with Behçet disease, and 21.1% in patients with sarcoidosis, so anti-UACA autoantibodies are considered as one of the autoantibodies in these panuveitis diseases. Originally, UACA was cloned from dog thyroid tissue following TSH stimulation, so we presumed UACA could be a novel candidate of autoantigen in autoimmune thyroid diseases [2]. Then, we analyzed the
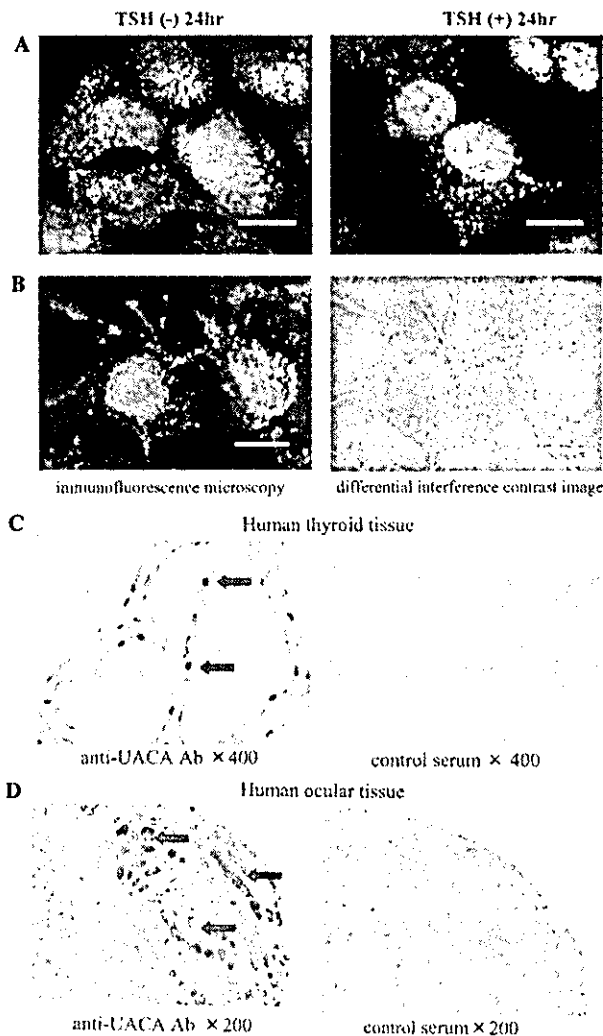
Fig. 3. (A) The cytochemical localization of UACA protein in FRTL5 cells in the absence or presence of TSH (1 mU/ml, 24 h). Inserted bar indicates 10 μm. (B) The fine cytochemical localization of UACA protein in FRTL5 cells followed by TSH stimulation (TSH 1 mU/ml, 24 h). Differential interference contrast image (right panel), and immunofluorescence microscopy image of FRTL5 cells (left panel). Inserted bar indicates10 μm. (C) The expression of UACA protein in human thyroid tissue of Graves' disease. Immunohistochemical analysis was done using rabbit anti-UACA antibodies. The sections were scanned at magnification (400×) using light microscopy. The arrows indicate nucleus of thyroid follicular cell expressing UACA protein. (D) The expression of UACA protein in human eye muscle tissue with Graves' ophthalmopathy. The sections were scanned at magnification (200×) using light microscopy. The arrows indicate eye muscle fibers expressing UACA proteins.

presence of anti-UACA antibodies in autoimmune thyroid diseases.

In ELISA study, the prevalence of anti-UACA antibodies in Graves' disease was significantly higher than that in healthy controls (15% vs. 0%). Moreover, the prevalence of anti-UACA antibodies in Graves' ophthalmopathy was significantly higher than that in

Graves' disease without ophthalmopathy (29% vs. 11%). We then investigated clinical manifestation of these patients with high UACA titer in detail. The prevalence of anti-UACA antibodies was 29% (9/31) in Graves' ophthalmopathy cases. These results clearly suggest that the appearance of anti-UACA antibody is strongly associated with eye muscle inflammation in patients with Graves' ophthalmopathy.

Thyroid-associated ophthalmopathy is considered to be an autoimmune disorder of eye muscle and surrounding orbital connective tissue and fat [3–7]. The eye symptoms associated with TAO can be classified into two subtypes, congestive ophthalmopathy (CO), in which inflammatory changes in periorbital tissues predominate, and ocular myopathy (OM), in which eye muscle is mainly damaged [30]. The current dogma tells that TAO is best explained by reactivity against thyroid and orbital tissue shared autoantigens [6,7]. One of such shared antigens is TSH receptor (TSHR), which is expressed in orbital preadipocytes. TSHR is mainly associated with the development of Graves' ophthalmopathy [8–11]. Several shared eye muscle and thyroid autoantigens have been investigated in eye muscle component in TAO, such as 63–67 kDa eye muscle membrane antigens and 55 kDa protein [12–24]. The flavoprotein (Fp) subunit of the mitochondrial enzyme succinate dehydrogenase is the so-called 64-kDa protein. Antibodies against Fp seem to be the best clinical marker of ophthalmopathy in patients with Graves' hyperthyroidism, and they are sensitive predictors for the development of eye muscle dysfunction in ophthalmopathy patients treated by antithyroid drugs [16,17]. The "55-kDa protein" was identified as G2s protein, eye muscle shared autoantigen with unknown function [22–24]. The primary reaction in eye muscle may be T-cell-mediated autoimmunity against TSHR of fibroblasts. The antibodies against Fp and G2s are produced secondary during the ophthalmopathy process, reflecting the release of sequestered cytoskeletal proteins from damaged eye muscles. Our observation indicates that UACA could be a novel candidate for thyroid and orbital shared autoantigen such as Fp in Graves' ophthalmopathy.

We also showed that UACA is expressed in eye muscle of patients with TAO as well as thyroid follicular cells in Graves' disease by immunohistochemical analysis. UACA was highly expressed in human eye muscle fibers of Graves' disease (Fig. 3D). This result indicates that UACA is simultaneously expressed in orbital eye muscle as well as thyroid follicular cells. High prevalence of anti-UACA antibodies is observed in patients with Graves' ophthalmopathy (Fig. 1). In particular, patients with severe ocular myopathy showed high UACA titer. Taken together, we presume that the appearance of anti-UACA antibodies could be a clinical marker for severe ocular myopathy, especially when its titer is high.

Wall and co-workers [16,17] suggested that anti-flavoprotein antibodies are produced by secondary immuno-regulatory event resulting from eye muscle necrosis. They also showed that the prevalence of anti-G2s antibodies was 50% in Graves' ophthalmopathy, and anti-G2s antibodies appear in early phase of TAO [22–24]. In our study, the prevalence of anti-UACA antibodies in Graves' ophthalmopathy is lower (29%) compared with anti-G2s antibodies. If UACA is the primary auto-antigen in Graves' ophthalmopathy, the prevalence should be higher. It is more likely that anti-UACA Ab is produced by secondary immunoregulatory process resulting from eye muscle necrosis like anti-flavoprotein antibodies. The low prevalence of anti-UACA Ab may raise the possibility that UACA is not relevant for the development of TAO. But, the prevalence of anti-UACA antibodies is only 20% in VKH disease, the original disease with anti-UACA antibodies. Because of the difficulty to produce recombinant UACA protein as a whole molecule (160 kDa), we used the C-terminal 18.0% portion of UACA to detect anti-UACA antibodies in patients' sera. A relatively lower prevalence of anti-UACA antibodies in Graves' patients may be due to the limited usage of C-terminal fragment of UACA protein for ELISA. To evaluate the presence of autoantibody against the whole UACA molecule, it is necessary to analyze patients' sera using other N-terminal fragments of UACA protein.

At present, the recognition of TSHR on the retro-ocular preadipocytes by TSHR autoantibodies and TSHR-specific T cells could be the initial event that drives the "homing" of the lymphocytes to the retro-orbital tissue. Then, the eye muscle inflammation is activated, resulting in the appearance of eye muscle autoantibodies including G2s, Fp, and UACA. Consequently, our observation about anti-UACA Ab is not contrary to this theory explaining the development of TAO. Since UACA is expressed in eye muscle, the appearance of anti-UACA antibodies may reflect immuno-logical damage of eye muscle fiber, as observed in flavoprotein. We presume that not thyroid destruction but eye muscle destruction is directly associated with the production of anti-UACA antibody. If we examine more TAO cases with anti-UACA antibodies, we can identify the clinical relevance of anti-UACA antibodies for the development of TAO.

Although the physiological function of UACA protein is still unclear, UACA contains six ankyrin repeats and coiled coil domains, including a motif of leucine zipper pattern. Ankyrin repeat is 31–33 amino acid motif present in a number of proteins and contributing to protein–protein interactions [31]. In FRTL5 thyroid cells, the amount of UACA protein increased in a time- and dose-dependent manner following TSH stimulation. In the absence of TSH, UACA protein was diffusely distributed both in nucleus and cytoplasm of FRTL5 cells.

Following TSH stimulation, UACA protein was exclusively recruited into nucleus of FRTL5 cell (Fig. 3A). Consequently, TSH augments UACA expression and simultaneously converts the localization of UACA within FRTL5 thyroid cells. Interestingly, UACA protein was highly expressed in nucleus of thyroid follicular cell in human thyroid tissue of Graves' disease. These results suggest that UACA protein may play a potential role for thyroid cell proliferation, since TSH drives the growth of thyroid follicular cells. Further study is necessary to reveal the physiological relevance of UACA in thyroid cell proliferation.

In summary, we demonstrate the high prevalence of anti-UACA autoantibodies in patients with Graves' disease. We confirmed that patients with Graves' ophthalmopathy (especially, with severe ocular myopathy) showed high UACA titer. UACA protein is expressed in autoimmune target tissues of Graves' disease, such as thyroid follicular cells and ocular eye muscles, indicating UACA is a novel thyroid–eye shared autoantigen. Although the sequence of autoantibodies production such as anti-G2s, anti-Fp or anti-UACA remains unknown, anti-UACA antibodies could be a clinical marker of ocular myopathy in patients with Graves' ophthalmopathy.

Acknowledgments

References

[1] K. Yamada, S. Senju, T. Nakatsura, Y. Murata, M. Ishihara, S. Nakamura, S. Ohno, A. Negi, Y. Nishimura, Identification of a novel autoantigen UACA in patients with panuveitis, Biochem. Biophys. Res. Commun. 280 (2001) 1169–1176.

[2] F. Wilkin, V. Savonet, A. Radulescu, J. Petermans, J.E. Dumont, C. Maenhaut, Identification and characterization of novel genes modulated in the thyroid of dogs treated with methimazole and propylthiouracil, J. Biol. Chem. 271 (1996) 28451–28457.

[3] J. Kiljanski, V. Nebes, J.R. Wall, The ocular muscle cell is a target of the immune system in endocrine ophthalmopathy, Proc. Int. Arch. Allergy. Immunol. 106 (1995) 204–212.

[4] A.M. McGregor, Has the autoantigen for Graves' ophthalmopathy been found?, Lancet 352 (1998) 595–596.

[5] A.P. Weetman, Thyroid-associated eye disease: pathophysiology, Lancet 338 (1991) 28–35.

[6] J.R. Wall, M. Salvi, N. Bernard, A. Boucher, D. Haegert, Thyroid-associated ophthalmopathy-A model for the association of organ-specific autoimmune disorder, Immunol. Today 12 (1991) 150–153.

[7] H.B. Burch, L. Wartofsky, Graves' ophthalmopathy: current concepts regarding pathogenesis and management, Endocrinol. Rev. 14 (1993) 747–793.

[8] F. Karlsson, P. Dahlberg, P. Jansson, K. Westermark, P. Enoksson, Importance of TSH receptor activation in the development of severe endocrine ophthalmopathy, Acta Endocrinol. 121 (1989) 132–141.

[9] R.S. Bahn, C.M. Dutton, N. Natt, W. Joba, C. Spitzweg, E.A. Heufelder, Thyrotropin receptor expression in Graves' orbital adipose/connective tissues: potential autoantigen in Graves' ophthalmopathy, J. Clin. Endocrinol. Metab. 83 (1998) 998–1002.

[10] R. Paschke, A. Metcalfe, L. Alcalde, G. Vassart, A. Weetman, M. Ludgate, Presence of nonfunctional thyrotropin receptor variant transcripts in retroocular and other tissues, J. Clin. Endocrinol. Metab. 79 (1994) 1234–1238.

[11] R.S. Bahn, Pathophysiology of Graves' ophthalmopathy: the cycle of disease, J. Clin. Endocrinol. Metab. 88 (2003) 1939–1946.

[12] M. Salvi, A. Miller, J.R. Wall, Human orbital tissue and thyroid membranes express a 64 kDa protein which is recognized by autoantibodies in the serum of patients with thyroid-associate ophthalmopathy, FEBS Lett. 232 (1988) 135–139.

[13] Y. Hiromatsu, M. Sato, K. Tanaka, S. Shoji, K. Nonaka, M. Chinami, H. Fukazawa, Significance of anti-eye muscle antibody in patients with thyroid-associated ophthalmopathy by quantitative Western blot, Autoimmunity 14 (1991) 1–8.

[14] Y-J. Wu, S.E.M. Clarke, P. Shepherd, Prevalence and significance of antibodies reactive with eye muscle membrane antigens in sera from patients with Graves' ophthalmopathy and other thyroid and nonthyroid disorders, Thyroid 8 (1998) 167–174.

[15] S. Kubota, K. Gunji, C. Stolarski, J.S. Kennerdell, J.R. Wall, Reevaluation of the prevalences of serum autoantibodies reactive with eye muscle antigens in patients with thyroid autoimmunity and ophthalmopathy, Thyroid 8 (1998) 175–179.

[16] S. Kubota, K. Gunji, B.A.C. Ackrell, B. Cochran, C. Stolarski, S. Wengrowicz, J.S. Kennerdell, Y. Hiromatsu, J. Wall, The 64-kDa eye muscle protein is the flavoprotein subunit of mitochondrial succinate dehydrogenase: the corresponding serum antibodies are good markers of an immune-medicated damage to the eye muscle in patients with Graves' hyperthyroidism, J. Clin. Endocrinol. Metab. 83 (1998) 433–447.

[17] K. Gunji, A. De Bellis, S. Kubota, J. Swanson, S. Wengrowicz, B. Cochran, B.A. Ackrell, M. Salvi, A. Bellastella, A. Bizzarro, A.A. Sinisi, J.R. Wall, Serum antibodies reactive against the flavoprotein subunit of succinate dehydrogenase are sensitive and specific markers of eye muscle autoimmunity in patients with Graves' hyperthyroidism, J. Clin. Endocrinol. Metab. 84 (1999) 16–22.

[18] Q. Dong, M. Ludgate, G. Vassart, Cloning and sequencing of a novel 64-kDa autoantigen recognized by patients with autoimmune thyroid disease, J. Clin. Endocrinol. Metab. 72 (1991) 1375–1381.

[19] A. Barsouk, S. Wengrowicz, D. Scalise, C. Stolarski, V. Nebes, M. Sato, J.R. Wall, New assays for the measurement of serum antibodies reactive with eye muscle membrane antigens confirm their significance in thyroid-associated ophthalmopathy, Thyroid 5 (1995) 195–200.

[20] T.C. Chang, T.J. Chang, Y.S. Huang, K.M. Hua, R.J. Su, S.C.S. Kao, Identification of autoantigen recognized by autoimmune ophthalmopathy sera with immunoblotting correlated with orbital computed tomography, Clin. Immunol. Immunopathol. 65 (1992) 161–166.

[21] M. Salvi, N. Bernard, A. Miller, Z.G. Zhang, E. Gardini, J.R. Wal, Prevalence of antibodies reactive with a 64 kDa eye muscle membrane antigen in thyroid-associated ophthalmopathy, Thyroid 1 (1991) 207–213.

[22] K. Gunji, A. De Bellis, A.W. Li, M. Yamada, S. Kubota, B. Ackrell, S. Wengrowicz, A. Bellastella, A. Bizzarro, A. Sinisi, J.R. Wall, Cloning and characterization of the novel thyroid and eye muscle shared protein G2s: autoantibodies against G2s are closely associated with ophthalmopathy in patients with Graves' hyperthyroidism, J. Clin. Endocrinol. Metab. 85 (2000) 1641–1647.

[23] M. Yamada, A.W. Li, K.A. West, C.H. Chang, J.R. Wall, Experimental model for ophthalmopathy in BALB/c and outbred (CD-1) mice genetically immunized with G2s and the thyrotropin receptor, Autoimmunity 35 (2002) 403–413.

[24] A. De Bellis, A. Bizzarro, M. Conte, C. Coronella, S. Solimeno, S. Perrino, D. Sansone, M. Guaglione, J.R. Wall, A. Bellastella, Relationship between longitudinal behavior of some markers of eye autoimmunity and changes in ocular findings in patients with Graves' ophthalmopathy receiving corticosteroid therapy, Clin. Endocrinol. (Oxf.). 59 (2003) 388–395.

[25] K.C. Ossoinig, The role of standardized echography in Graves' disease, Acta Ophthalmol. (Copenh) 204 (1992) 81.

[26] X.P. Pang, J.M. Hershman, M. Chung, A.E. Pekary, Characterization of tumor necrosis factor-α receptors in human and rat thyroid cells and regulation of the receptors by thyrotropin, Endocrinology 125 (1989) 1783–1788.

[27] T. Ito, T. Seyama, T. Hayashi, K. Dohi, T. Mizuno, K. Iwamoto, N. Tsuyama, N. Nakamura, M. Akiyama, Establishment of two human thyroid carcinoma cell lines (8305C, 8505C) bearing p53 gene mutations, Int. J. Oncol. 4 (1994) 583–586.

[28] M. Derwahl, M. Kuemmel, P. Goretzki, H. Schatz, M. Broecker, Expression of the human TSH receptor in a human thyroid carcinoma cell line that lacks an endogenous TSH receptor, Biochem. Biophys. Res. Commun. 191 (1993) 1131–1138.

[29] J.A. Fagin, K. Matsuo, A. Karmakar, D.L. Chen, S.H. Tang, H.P. Koeffler, High prevalence of mutations of the p53 gene in poorly differentiated human thyroid carcinomas, J. Clin. Invest. 91 (1993) 179–184.

[30] T.P. Solovyeva, Endocrine ophthalmopathies. Problems of rational classification, Orbit 3 (1989) 193–198.

[31] S.E. Lux, K.M. John, V. Bennett, Analysis of cDNA for human erythrocyte ankyrin indicates a repeated structure with homology to tissue-differentiation and cell-cycle control proteins, Nature 344 (1990) 36–42.

Comparison of Frequency of Interferon-γ-Positive CD4+ T Cells Before and After Percutaneous Coronary Intervention and the Effect of Statin Therapy in Patients With Stable Angina Pectoris

Tomoko Tanaka, MD, Hirofumi Soejima, MD, PhD, Nobutaka Hirai, MD, PhD,
Tomohiro Sakamoto, MD, PhD, Michihiro Yoshimura, MD, PhD, Ichiro Kajiwara, MD,
Yuji Miyao, MD, PhD, Kazuteru Fujimoto, MD, PhD, Hiroo Miyagi, MD, PhD,
Atsushi Irie, PhD, Yasuharu Nishimura, MD, PhD, and Hisao Ogawa, MD, PhD

We investigated the effect of statin therapy on T-cell activation in patients who underwent percutaneous coronary intervention by using flow cytometric analysis. The increased frequency of interferon-γ-positive CD4+ T cells after percutaneous coronary intervention was significant in the group treated without statins but not in the group treated with statins. ©2004 by Excerpta Medica, Inc.

(Am J Cardiol 2004;93:1547-1549)

Atherosclerosis has been demonstrated to be an inflammatory process involving various immune cells,[1] in particular T cells and macrophages in plaque.[2] Another study using flow cytometry has shown that activated T cells are related to plaque instability. Liuzzo et al[3] measured the frequency of activated T cells treated with phorbol myristate acetate and ionomycin. We recently reported a significant increase in activated T cells in patients with unstable angina.[4] In addition, percutaneous coronary intervention (PCI) has been shown to induce an inflammatory response locally[5] and systemically,[6] and hydroxymethyl-glutaryl-coenzyme A reductase inhibitors (statins) have been found to affect inflammation.[7] In other research, clinical trials have shown that statins decrease the incidence of early death and recurrent ischemia in patients undergoing PCI.[8] Therefore, we investigated the effect of statin therapy on T-cell activation in patients who underwent PCI using flow cytometric analysis.

• • •

The study population consisted of 41 consecutive

TABLE 1 Clinical Characteristics of Statin-Treated Group and Non–Statin-Treated Group

Variable	Statin Treatment	
	+ (n = 17)	0 (n = 24)
Age (yrs)	69 ± 8	73 ± 7
Men	9 (53%)	15 (63%)
Body mass index (kg/cm²)	24.2 ± 2.3	23.1 ± 3.2
Total cholesterol (mg/dl)	205 ± 53	201 ± 43
Triglyceride (mg/dl)	144 ± 57	120 ± 46
HDL cholesterol (mg/dl)	47 ± 8	49 ± 17
LDL cholesterol (mg/dl)	135 ± 50	126 ± 28
Diabetes mellitus	6 (35%)	7 (29%)
Systemic hypertension	14 (82%)	21 (88%)
Smoker	4 (24%)	5 (21%)
No. of coronary arteries narrowed ≥75% in diameter		
1	6 (35%)	10 (42%)
2	10 (59%)	10 (42%)
3	1 (6%)	4 (17%)
Stent implantation	12 (71%)	20 (83%)
Medications		
Aspirin	15 (88%)	22 (92%)
ACE inhibitors	3 (18%)	5 (21%)
Calcium antagonist	12 (71%)	16 (67%)
β Blockers	3 (18%)	5 (21%)
Nitrates	4 (24%)	6 (25%)

Data are presented as mean ± SD or number of patients (percents).
ACE = angiotensin-converting enzyme; HDL = high density lipoprotein; LDL = low density lipoprotein.

patients (24 men and 17 women; mean age 72 ± 7 years) with stable angina pectoris who underwent elective single-vessel PCI between July 2002 and June 2003. Exclusion criteria were inflammatory disease, collagen disease, infection, unstable angina, acute myocardial infarction, and heart failure. The patients were assigned to 1 of 2 groups depending on whether statins were administered before admission: statin-treated group or non–statin-treated group. Informed consent was obtained from each patient.

PCI was performed according to a standard technique in 1 vessel per patient. All patients received an intravenous injection of 5,000 IU of heparin and intracoronary injection of isosorbide dinitrate during angioplasty, in which a balloon was positioned at the stenotic region and inflated. Adjunctive stent implantation was performed if the residual diameter stenosis
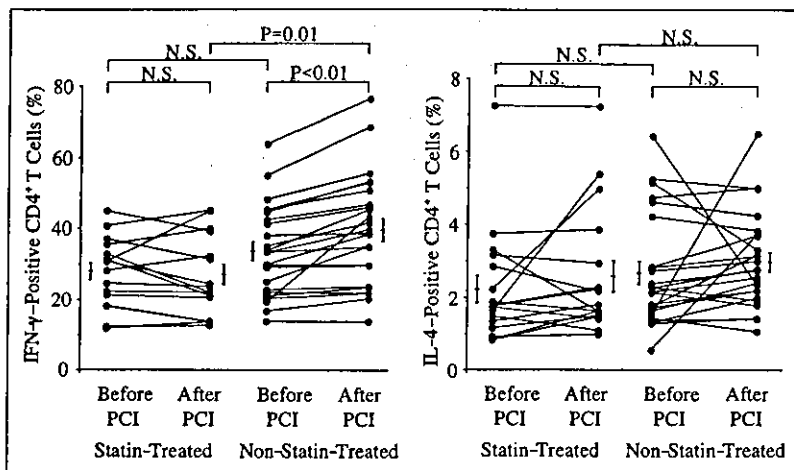
FIGURE 1. Frequency of IFN-γ–positive *(left)* and interleukin-4 (IL-4)–positive *(right)* CD4$^+$ T cells before and after PCI (mean ± SE).

was ≥30% and there was a complex coronary dissection. All PCI procedures were successful.

Peripheral blood samples were obtained with a 21-gauge needle through clean vein puncture from all patients on admission for the measurement of lipid levels. Whole blood samples were also taken before PCI and 2 days after PCI for measurement of interferon-γ (IFN-γ)–positive CD4$^+$ T-cell frequencies. For each sample, 3 ml of blood was drawn into a heparinized Vacutainer.

Whole blood was incubated at 37°C and in 5% carbon dioxide for 4 hours in nonactivating medium (RPMI 1640 supplemented with 10% fetal calf serum and 40 μg/ml of brefeldin A; Sigma Chemical Co., St. Louis, Missouri) or activating medium (nonactivating medium with 40 ng/ml of phorbol myristate acetate [Calbiochem, San Diego, California] and 4 μg/ml of ionomycin [Sigma Chemical Co.]). After being washed with ice-cold phosphate buffered saline, cells were recovered by centrifugation and adjusted to 5 × 10^5 white blood cells per test. Cell surfaces were stained with anti-CD4-Cy-Chrome monoclonal antibody (BD Pharmingen, San Jose, California), and fixation and permeabilization were performed with IntraPrep reagent (Beckman Coulter, Hialeah, Florida). Intracellular cytokines were stained with anti-IFN-γ fluorescein isothiocyanate monoclonal antibody and anti–interleukin-4 phycoerythrin monoclonal antibody (Beckman Coulter). IFN-γ–positive CD4$^+$ T cells and interleukin-4–positive CD4$^+$ T cells were analyzed using 3-color flow cytometry with the FACScan cytometer and CellQuest software (Becton Dickinson). Nonspecific staining with the isotype-matched control monoclonal antibody was <1%.

Continuous values were expressed as mean ± SD and were compared with unpaired *t* test. Categorical data were expressed as frequencies and percentages. Chi-square test was used for the analysis of categorical data. Changes in frequencies of IFN-γ–positive CD4$^+$ T cells before and after PCI were compared with the Wilcoxon signed-ranks test. Differences in

these frequencies between the statin-treated and non–statin-treated groups were compared with the Mann-Whitney U test. A p value <0.05 was considered statistically significant.

Twenty-four of the 41 patients were assigned to the non–statin-treated group and the remaining 17 were assigned to the statin-treated group. Nine patients were treated with pravastatin, 4 patients with atorvastatin, and 4 patients with simvastatin. Clinical characteristics of the statin-treated group and the non–statin-treated group are listed in Table 1. There was no significant difference between the 2 groups with respect to characteristics and medications.

After PCI, the frequency of IFN-γ–positive CD4$^+$ T cells increased significantly from 33.64 ± 12.66% to 39.63 ± 15.42% in the non–statin-treated group (p <0.01). The frequency increased in 22 of 24 patients in the non–statin-treated group. In contrast, frequency after PCI did not significantly change (from 28.10 ± 9.68% to 27.06 ± 11.32%) in the statin-treated group. The frequency increased in 7 of 17 patients in the statin-treated group (Figure 1). The change in the frequency of interleukin-4–positive CD4$^+$ T cells was not significant in the statin-treated group or the non–statin-treated group.

• • •

The results of the present study showed that the frequency of IFN-γ–positive CD4$^+$ T cells significantly increased in the non–statin-treated group after PCI. The frequency after PCI increased in 22 of 24 patients in the non–statin-treated group. Conversely, the frequency did not significantly change in the statin-treated group. The frequency increased in 7 of 17 patients in the statin-treated group. The frequency decreased in the remaining 10 patients. Changes in frequency of interleukin-4–positive CD4$^+$ T cells in the statin-treated and the non–statin-treated groups between before and after PCI were not significant.

PCI induces an inflammatory response locally and systemically.[9] PCI causes plaque rupture, hemorrhage, arterial wall damage, and release of inflammatory factors with leukocyte and platelet activation.[10] A positive association between invasion of T cells and recurrence of unstable angina after PCI has also been found.[11] These findings agree with our observation of a significant increase in T-cell activation after PCI in the non–statin-treated group. Statins have been found to provide early benefits in patients undergoing PCI.[12] Experimental studies have supported the view that statins reduce inflammation[13] and that treatment with statins decreases the number of inflammatory cells in atherosclerotic plaques.[14] In an in vitro study, Kwak et al[15] observed that statin treatment inhibited T-cell proliferation and differentiation through decreased expression of major histocompatibility complex II

mRNA, and Weitz-Schmidt et al[16] reported that several statins impaired T-cell stimulation by directly binding to the lymphocyte function-associated antigen-1 regulatory site on leukocytes. Further, Youssef et al[17] recently demonstrated that statins suppressed secretion of IFN-γ from T cells in experimental autoimmune encephalomyelitis. In the present study, statins decreased T-cell activation after PCI, which correlates with published results.

1. Libby P. Inflammation in atherosclerosis. *Nature* 2002;420:868–874.
2. Hansson GK. Immune mechanisms in atherosclerosis. *Arterioscler Thromb Vasc Biol* 2001;21:1876–1890.
3. Liuzzo G, Kopecky SL, Frye RL, O'Fallon WM, Maseri A, Goronzy JJ, Weyand CM. Perturbation of the T-cell repertoire in patients with unstable angina. *Circulation* 1999;100:2135–2139.
4. Soejima H, Irie A, Miyamoto S, Kajiwara I, Kojima S, Hokamaki J, Sakamoto T, Tanaka T, Yoshimura M, Nishimura Y, Ogawa H. Preference toward a T-helper type 1 response in patients with coronary spastic angina. *Circulation* 2003;107:2196–2200.
5. Serrano CV Jr, Ramires JA, Venturinelli M, Arie S, D'Amico E, Zweier JL, Pileggi F, da Luz PL. Coronary angioplasty results in leukocyte and platelet activation with adhesion molecule expression. Evidence of inflammatory responses in coronary angioplasty. *J Am Coll Cardiol* 1997;29:1276–1283.
6. Azar RR, McKay RG, Kiernan FJ, Seecharran B, Feng YJ, Fram DB, Wu AH, Waters DD. Coronary angioplasty induces a systemic inflammatory response. *Am J Cardiol* 1997;80:1476–1478.
7. Plenge JK, Hernandez TL, Weil KM, Poirier P, Grunwald GK, Marcovina SM, Eckel RH. Simvastatin lowers C-reactive protein within 14 days: an effect independent of low-density lipoprotein cholesterol reduction. *Circulation* 2002;106:1447–1452.

8. Serruys PW, de Feyter P, Macaya C, Kokott N, Puel J, Vrolix M, Branzi A, Bertolami MC, Jackson G, Strauss B, Meier B. Fluvastatin for prevention of cardiac events following successful first percutaneous coronary intervention: a randomized controlled trial. *JAMA* 2002;287:3215–3222.
9. Inoue T, Uchida T, Yaguchi I, Sakai Y, Takayanagi K, Morooka S. Stent-induced expression and activation of the leukocyte integrin Mac-1 is associated with neointimal thickening and restenosis. *Circulation* 2003;107:1757–1763.
10. Farb A, Sangiorgi G, Carter AJ, Walley VM, Edwards WD, Schwartz RS, Virmani R. Pathology of acute and chronic coronary stenting in humans. *Circulation* 1999;99:44–52.
11. Arbustini E, De Servi S, Bramucci E, Porcu E, Costante AM, Grasso M, Diegoli M, Fasani R, Morbini P, Angoli L, et al. Comparison of coronary lesions obtained by directional coronary atherectomy in unstable angina, stable angina, and restenosis after either atherectomy or angioplasty. *Am J Cardiol* 1995;75:675–682.
12. Chan AW, Bhatt DL, Chew DP, Quinn MJ, Moliterno DJ, Topol EJ, Ellis SG. Early and sustained survival benefit associated with statin therapy at the time of percutaneous coronary intervention. *Circulation* 2002;105:691–696.
13. Rezaie-Majd A, Prager GW, Bucek RA, Schernthaner GH, Maca T, Kress HG, Valent P, Binder BR, Minar E, Baghestanian M. Simvastatin reduces the expression of adhesion molecules in circulating monocytes from hypercholesterolemic patients. *Arterioscler Thromb Vasc Biol* 2003;23:397–403.
14. Crisby M, Nordin-Fredriksson G, Shah PK, Yano J, Zhu J, Nilsson J. Pravastatin treatment increases collagen content and decreases lipid content, inflammation, metalloproteinases, and cell death in human carotid plaques: implications for plaque stabilization. *Circulation* 2001;103:926–933.
15. Kwak B, Mulhaupt F, Myit S, Mach F. Statins as a newly recognized type of immunomodulator. *Nat Med* 2000;6:1399–1402.
16. Weitz-Schmidt G, Welzenbach K, Brinkmann V, Kamata T, Kallen J, Bruns C, Cottens S, Takada Y, Hommel U. Statins selectively inhibit leukocyte function antigen-1 by binding to a novel regulatory integrin site. *Nat Med* 2001;7:687–692.
17. Youssef S, Stuve O, Patarroyo JC, Ruiz PJ, Radosevich JL, Hur EM, Bravo M, Mitchell DJ, Sobel RA, Steinman L, Zamvil SS. The HMG-CoA reductase inhibitor, atorvastatin, promotes a Th2 bias and reverses paralysis in central nervous system autoimmune disease. *Nature* 2002;420:78–84.

Risk Factors and Outcomes in Patients With Coronary Artery Aneurysms

Timir S. Baman, MD, Jason H. Cole, MD, Chandan M. Devireddy, MD, and Laurence S. Sperling, MD

Previous small series have provided conflicting data on the association between coronary artery aneurysms and traditional cardiac risk factors, as well as limited information on patient outcomes. This investigation sought to determine whether the presence of coronary artery aneurysms has an adverse affect on patient outcomes. The results show that coronary aneurysms were an independent predictor of mortality, and overall 5-year survival in patients with aneurysms was only 71%. We believe that clinicians should aggressively monitor and modify coronary risk factors in patients with coronary aneurysms. ©2004 by Excerpta Medica, Inc.

(Am J Cardiol 2004;93:1549–1551)

M any questions exist regarding clinical risk factors and long-term prognosis of patients with coronary aneurysms exist. Multivariate analysis of coronary aneurysms as a correlate of long-term mortality has not been done in a large series. To better study this issue, we identified a large population with coronary aneurysms documented by strict angiographic criteria.

• • •

Information on all patients who underwent coronary angiography at Emory University Hospitals between 1995 and 2003 were included in a cardiac database. Patient variables recorded were gender, age, hypertension (defined by current or previous therapy or a history of blood pressure >140/95 mm Hg), history of coronary artery disease (CAD), smoking history, hyperlipidemia (per previous diagnosis), and history of and type of diabetes mellitus. Diabetes was defined by ongoing oral or insulin therapy or diet control, provided the clinician also had laboratory evidence of hyperglycemia. Follow-up data were obtained by telephone interview and hospital encounters.

All patients with the terms "coronary aneurysm" or "coronary ectasia" in their catheterization reports were

Identification of systemically expanded activated T cell clones in MRL/lpr and NZB/W F1 lupus model mice

G. ZHOU*†, K. FUJIO*, A. SADAKATA*, A. OKAMOTO*, R. YU* & K. YAMAMOTO** *Department of Allergy and Rheumatology, Graduate School of Medicine, the University of Tokyo, Tokyo, Japan, and †Department of Rheumatology and Nephrology, China-Japan Union Hospital of Ji Lin University, Changchun, China

SUMMARY

CD4⁺ T lymphocytes play an important role in the pathogenesis of systemic lupus erythematosus (SLE). To characterize the clonal expansion of CD4⁺ T cells in murine lupus models, we analysed the T cell clonality in various organs of young and nephritic MRL/lpr and NZB/W F1 mice using reverse transcription–polymerase chain reaction (RT-PCR) and subsequent single-strand conformation polymorphism (SSCP) analysis. We demonstrated that some identical T cell clonotypes expanded and accumulated in different organs (the bilateral kidneys, brain, lung and intestine) in nephritic diseased mice, and that a number of these identical clonotypes were CD4⁺ T cells. In contrast, young mice exhibited little accumulation of common clones in different organs. The T cell receptor (TCR) Vβ usage of these identical clonotypes was limited to Vβ2, 6, 8·1, 10, 16 and 18 in MRL/lpr mice and to Vβ6 and 7 in NZB/W F1 mice. Furthermore, some conserved amino acid motifs such as I, D or E and G were observed in CDR3 loops of TCRβ chains from these identical CD4⁺ clonotypes. The existence of systemically expanding CD4⁺ T cell clones in the central nervous system (CNS) suggests the involvement of the systemic autoimmunity in CNS lesions of lupus. FACS-sorted CD4⁺CD69⁺ cells from the kidney displayed expanded clonotypes identical to those obtained from the whole kidney and other organs from the same individual. These findings suggest that activated and clonally expanded CD4⁺ T cells accumulate in different tissues of nephritic lupus mice, and these clonotypes might recognize restricted T cell epitopes on autoantigens involved in specific immune responses of SLE, thus playing a pathogenic role in these lupus mice.

Keywords animal models/ studies – mice/ rats lupus/ systemic lupus erythematosus T cell receptor (TCR)

INTRODUCTION

Systemic lupus erythematosus (SLE) is an autoimmune disease characterized by the production of pathogenic autoantibodies and tissue deposition of immune complexes, which results in multiple organ damage. MRL/lpr and NZB/W F1 mice, that develop spontaneously a lupus syndrome closely resembling human SLE, are considered to be excellent models for investigating the pathogenesis of the human disease. It has been suggested that T cell-dependent antigen-specific immune responses play a key role in the pathogenesis of these two strains. Published data have documented the involvement of T cells, especially CD4⁺ T cells, in lupus in the mouse. This involvement includes: (1) the infiltration of affected tissues with predominantly CD4⁺ T cells [1,2]; (2) the

development of lymphadenopathy but not autoimmune renal disease or autoantibodies in CD4⁺ T cell-deficient or MHC class II-deficient lupus mice [3,4]; and (3) improvement in the disease manifestations following treatment with anti-CD4 MoAb [5–7]. These results suggest that CD4⁺ T cells play an important role in the development of lupus.

Most of the studies have implicated CD4⁺ T cells as primarily responsible for pathogenic anti-DNA autoantibody production [3,8,9]. Although the participation and importance of CD4⁺ T cells in lupus mice has been emphasized, the pathogenic CD4⁺ T cell clonotypes that expanded in different sites of these murine models have not yet been identified and characterized. Also, the nature of antigen-specific T cells in SLE still remains poorly defined. Detection and characterization of the pathogenic T cell clonotypes that expanded in lupus mice may help to illustrate the contribution of CD4⁺ T cell clones to the antigen-specific immune responses in SLE and provide insight into the nature of the T cell Ags involved.

In order to address these questions and to investigate further the pathogenic role of CD4⁺T cells clonally expanded in SLE, we compared the T cell clonality in different organs derived from young and nephritic NZB/W F1 as well as MRL/lpr mice using the established reverse transcription–polymerase chain reaction (RT-PCR)–single-strand conformation polymorphism (SSCP) study in combination with CDR3 sequence analysis of the T cell receptor (TCR) Vβ family. Our results showed that there were some identical T cell clonotypes expanded and accumulated in different organs in nephritic mice. Most of those identical clonotypes were CD4⁺ T cells. In contrast, few identical T cell clonotypes were found in young mice. In addition, some conserved amino acid motifs were observed in CDR3 loops of TCR Vβ from these identical CD4⁺ clonotypes.

MATERIALS AND METHODS

Mice

NZB/W F1 mice were purchased from Japan SLC (Shizuoka, Japan) and MRL/lpr mice were purchased from Charles River (Kanagawa, Japan). All the mice used were female. Female MRL/lpr mice develop severe nephritis at 12–24 weeks, and female NZB/W F1 mice develop severe nephritis at 24–48 weeks. Therefore, we selected 20–26-week-old MRL/lpr mice and 36–47-week-old NZB/W F1 mice with severe glomerulonephritis (continuous proteinuria > 300 mg/dl) accompanied by symptoms related to the central nervous system as nephritic mice. Six-week-old MRL/lpr mice and 12-week-old NZB/WF1 mice were used as young mice.

RNA isolation and cDNA synthesis

The spleen, peripheral lymph nodes (pLNs: axillary, inguinal and mesenteric), kidneys, brain, lung, small intestine and heart were collected from each mouse after perfusion of the mice with PBS of 20 ml. Total RNA was isolated from the above tissues using ISOGEN (Nippon Gene, Tokyo, Japan) according to the manufacturer's protocol. Eight to 10 μg of total RNA was converted to cDNA.

TCR RT-PCR/single-strand conformation polymorphism (SSCP) analysis

RT-PCR–SSCP studies of the TCR Vβ chain were performed as described previously [10,11]. Briefly, one-fiftieth of each cDNA reaction was mixed with each primer set (a common Cβ primer and a Vβ specific primer) at a final concentration of 1·2 pmol/l. PCRs were performed with dNTPs and Taq DNA polymerase (Takara Bio Inc, Shiga, Japan) for 35 cycles (95°C for 1·5 min, 54°C for 2 min and 72°C for 3 min) in a GeneAmp⁹ PCR System 9700 (Applied Biosystems, Foster City, CA, USA). After electrophoresis in non-denaturing 4% polyacrylamide gels, the amplified product was transferred onto a nylon membrane (Perkin Elmer Co. Foster City, CA, USA) and then hybridized with a biotinylated Cβ oligonucleotide probe. Finally, the membrane was visualized by subsequent incubation with streptoavidin, biotinylated alkaline phosphatase and a chemiluminescent substrate system (Phototope™ Star Detection kit; New England Biolabs, Beverley, MA, USA).

Identification of TCR CDR3 for sequencing analysis

Representative subcloned DNA with different CDR3 sequences and RT-PCR products for each organ were subjected to SSCP electrophoresis at the same time to determine which of the T cell

clonotypes with unique TCR Vβ CDR3 sequences migrate to the position on the gel where the discrete band of interest was shown by the former PCR product. Identified DNAs were then sequenced by an ABI 310 automated sequencer (Applied Biosystems, Foster City, CA, USA).

Preparation of single cell suspension

The spleen, kidneys, lung or peripheral lymph nodes (pLNs; axillary, inguinal and mesenteric) derived from the mice were minced and incubated in 5 ml of an enzyme preparation containing RPMI-1640 (Gibco Laboratories, Grand Island, NY, USA), 10% fetal calf serum, 1% penicillin, 0·1% collagenase and 20 μg/ml DNase (Sigma Chemical Co., St Louis, MO, USA) at 37°C for 30 min to obtain single cell suspensions.

Magnetic cell sorting

Single cell suspensions from pLNs were separated into CD4 depletion, CD8 depletion or CD4 and CD8 depletion populations using MACS® magnetic separation columns LD (Miltenyi Biotec, Bergisch Gladbach, Germany) according to the manufacturer's instructions. In brief, cells were incubated with biotin-conjugated rat antimouse CD4 (PharMingen; clone RM4-5), biotin-conjugated rat antimouse CD8α (PharMingen; (clone 53–6·7)), or both of these antibodies for 10 min on ice, followed by Streptavidin MicroBeads (Miltenyi Biotec) for 15 min at 4°C. After washing, the mixtures of labelled and non-labelled cells were passed over an LD column inserted into a MidiMACS magnet (Miltenyi Biotec). The CD4-, CD8- or CD4- and CD8-depleted fraction was collected in the flow-through. The purity of the MACS-separated depletion population confirmed by flow cytometry was >94%.

Flow cytometric analysis and antibodies

For single cells obtained from the lung or kidneys of young and nephritic NZB/W F1 mice, the following MoAbs used for immunofluorescent staining were purchased from BD PharMingen (San Diego, CA, USA): FITC anti-mouse CD4 (GK1·5), PE anti-mouse CD69 (H1·2F3) and PE antimouse CD62L (MEL-14). After washing in 1 × phosphate buffered saline (PBS), cells were fixed with 1% paraformaldehyde in PBS and then stored at 4°C in the dark before flow cytometric analysis. Cytometry was performed on an EPICS XL Flow Cytometer (Coulter Electronics, Hialeah, FL, USA) using SYSTEM II™ software version 2·1 (Becton Dickinson). The gate was set for lymphocyte based on forward and side light-scatter characteristics, and 10 000 events were acquired per sample.

FACS purification of cell populations

Single cells prepared from the right kidney of nephritic NZB/W F1 mice were stained with FITC anti-CD4 MoAb, PE anti-CD40L MoAb and biotin anti-CD69 followed by allophycocyanin-conjugated streptavidin. Then CD4⁻CD69⁺ cells were sorted on a FACSVantage HG flow cytometer (Becton Dickision) after being gated on a CD4-positive population. The purity of the sorted population exceeded 97%.

RESULTS

Analyses of T cell clonality in various organs from young and nephritic murine models of lupus

To compare the expanded T cell clonality in various organs from nephritic mice with lupus nephritis and young mice without obvi-

ous proteinuria, we performed the established RT-PCR–SSCP analysis which can discriminate T cell clones with different T cell receptor (TCR) Vβ motifs. The spleen, peripheral lymph nodes, bilateral kidneys, brain, lung, small intestine and heart were isolated from young and nephritic MRL/lpr or NZB/W F1 mice and were subjected to RT-PCR–SSCP analysis as described in Materials and Methods. Representative results are shown in Fig. 1. Although young lupus-prone mice without any manifestation of nephritis showed a few distinct expanded T cell clones in each individual organ, these clones were essentially restricted to the individual organ. In contrast, dominant T cell clonal expansions and accumulations with some limited TCR Vβ usage were observed in the kidneys and other organs of nephritic diseased mice, and intriguingly some identical clonotypes were demonstrated in the bilateral kidneys, brain, lung and intestine. The dominant T cell clonal expansions were essentially conserved in repeated electrophoresis of the new PCR products sythesized from the same cDNAs. The limited TCR Vβ usage was Vβ2, Vβ6, Vβ8·1, Vβ10, Vβ16, Vβ18 in MRL/lpr mice (Fig. 1a) and Vβ6, Vβ7 in NZB/W F1 mouse (Fig. 1b).

To further determine the phenotype of clonally expanded and accumulated T cells in different tissues of nephritic mice, isolated pLNs were separated into CD4-depleted, CD8-depleted or CD4- and CD8-depleted populations using the magnetic cell sorting method (MACS), and were then subjected to RT-PCR–SSCP analysis. A number of these commonly expanded T cell clonotypes were of the CD4+ subset both in the NZB/W F1 and MRL/lpr mice, as many of these clonotypes disappeared upon CD4 or CD4·CD8 depletion. This is consistent with the FACS results, in which the percentages of CD4+ T cells in organs were found to be about two to three times higher than the percentages of CD8+ T cells (data not shown). In Fig. 1a, some bands of CD4·CD8 depletion exhibited a pattern similar as after CD8 depletion. Since we have confirmed the depletion of each of CD4, CD8 or CD4·8 depletion by FACS analysis, the residual bands in CD4·8 depletion seem to be derived from CD4⁻CD8⁻CD3⁺ cells accumulated in nephritic MRL/lpr mice [12]. Many of the residual bands in CD4·8 depletion did not showed commonly expansion in organs. These results indicate that the commonly expanded T cell clones exist in different tissues in the nephritic mice, and that a number of these identical clonotypes belong to the CD4+ subset.

TCR Vβ CDR3 sequence analysis

We next tried to examine whether these commonly expanded CD4+T cell clonotypes in various organs of NZB/W F1 and MRL/lpr mice share some characteristics of the CDR3 sequences with the TCR Vβ chains. RT-PCR products of TCR Vβ6 genes of the kidney and brain from nephritic mice of these two strains were cloned and sequenced. Then the representative PCR products of plasmid DNA with different CDR3 sequences were subjected to SSCP electrophoresis with the former TCR Vβ6 PCR product. We determined which of the T cell clonotypes with unique CDR3 sequences migrate to the same position on gel as the designated identical bands in the analyses of various organs. The CDR3 sequence of these identical TCR Vβ6 clonotypes was thus determined. As shown in Fig. 2, the indicated bands with the same migration from the left kidney and brain in the same individual exhibited an identical CDR3 sequence. These TCR Vβ6 chains displayed a common amino acid residue motif of IXD in CDR3 loops from two different individuals of NZB/W F1 mice. Similarly, IXD was also found in one MRl/lpr mouse, and I and E was found

in another. The amino acid of G was shown in three individuals of these two strains. These N(D)N regions encoding isoleucine gave rise to the sequence CASSI in TCR Vβ6 gene. These data strongly suggest an antigen-driven response in these commonly expanded CD4+ T cells.

Phenotypic analysis of CD4+ T cells in nephritic NZB/W F1 mice

To demonstrate whether the CD4+T cells that accumulated in different tissues were activated, we performed a FACS analysis of some activation markers expressed on CD4+T cells in the spleen, kidney, lung and small intestine of nephritic NZB/W F1 mice. As can be seen in Table 1, the existence of CD69+CD4+ and CD62L^low CD4+ T cell populations were found in CD4+ T cells derived from the spleen, kidney, lung and small intestine. These findings indicated that the CD4+T cells that accumulated in nephritic NZB/W F1 mice were activated.
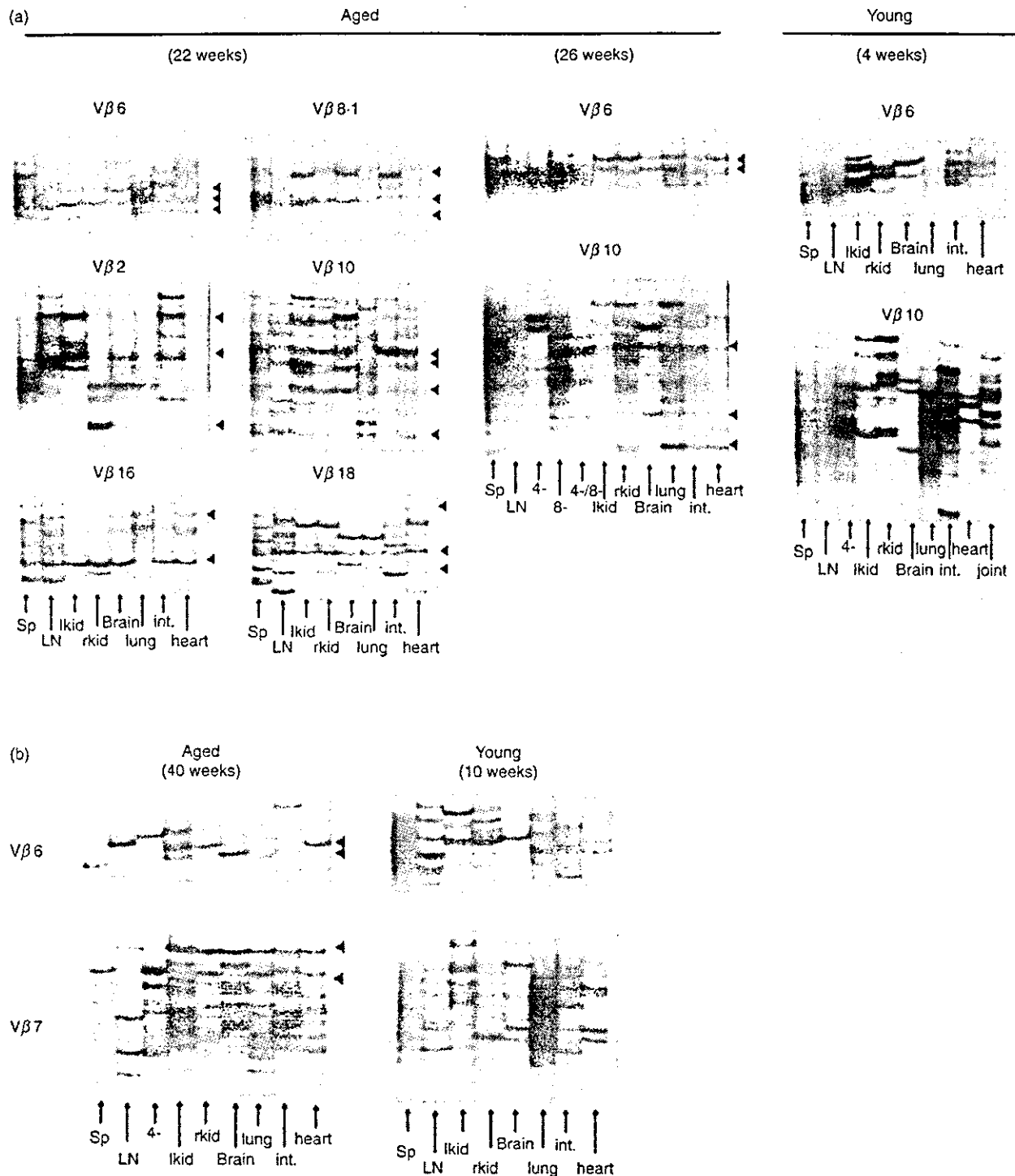
Phenotype of T cell clone commonly expanded in various organs

To investigate which phenotypes of the activated CD4+ T cells were involved in the common expanding in various organs, we purified CD4+CD69+ cells from the right kidney of a 47-week-old NZB/W F1 mouse by cell sorting on a FACSVantage. Total RNA of the sorted cells was extracted, reverse transcribed and amplified with primers specific for Vβ6 and Vβ7. Subsequent SSCP analysis was then carried out to compare the expanded clonotype of the sorted CD4+CD69+ population with that of the whole T cell populations in other tissues, including the left kidney. As presented in Fig. 3, the CD4+CD69+ cell population displayed expanded bands identical to those of the left kidney and other different tissues with respect either to Vβ6 or Vβ7. The strong identity of the SSCP electrophoresis pattern of the left and right kidneys (Fig. 1a and b) and left kidney and CD4+CD69+ sorted cells from the right kidney (Fig. 3) suggest the reproducibility of our SSCP analysis. These findings revealed that the commonly expanded T cell clonotypes in various organs in this lupus model have an activated phenotype.
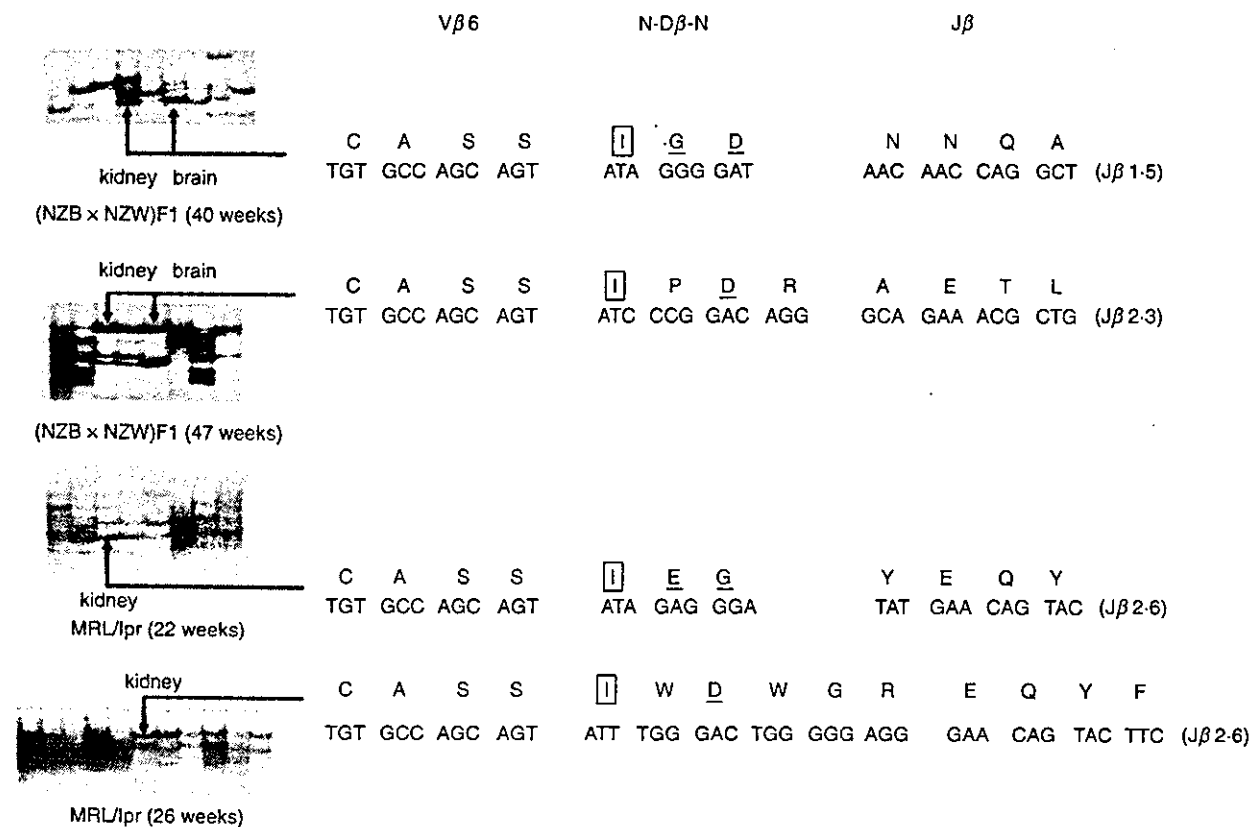
DISCUSSION

RT-PCR–SSCP analysis is thought to be one of the most sensitive techniques for detecting expanded and accumulated T cell clones *in vivo* and *in vitro* [13–15]. In the present study, we employed this method to investigate the pathogenic role of CD4+ T cells in SLE by comparing T cell clonality in various organs obtained from young and nephritic mice of the MRL/lpr and NZB/W F1 strains. Our results demonstrated that although young mice of these two strains showed a few distinct expanded T cell clones, no identical clonotypes were found among the different organs. In contrast, some identical T cell clonotypes with limited TCR Vβ usage showed expansion and accumulation in different organs taken from nephritic mice. These observations indicate the systemic nature of this disease and the possible pathogenic T cell clonotypes involved in these two strains as well. Moreover, these identical clonotypes were mainly CD4+ T cells, suggesting that there is selective expansion and accumulation of the CD4+ subset at different sites, and that these clonally expanded CD4+ T cells may play a dominant role in the disease development in these lupus mice.

Previous studies have revealed that in contrast to CD8+ and CD4⁻CD8⁻ T cells, a number of CD4+ T cells showed a large disease-related increase in NZB/W F1 mice [1]. Also, in addition to

(a)

Aged   Young

(22 weeks)   (26 weeks)   (4 weeks)

Vβ6   Vβ8-1   Vβ6   Vβ6

Vβ2   Vβ10   Vβ10   Vβ10

Vβ16   Vβ18

(b)

Aged (40 weeks)   Young (10 weeks)

Vβ6

Vβ7

Fig. 1. Analysis of T cell clonality in various organs from young and nephritic lupus mice by RT-PCR–SSCP. Different organs such as the spleen, LNs, bilateral kidneys, brain, lung, small intestine and heart isolated using the magnetic cell sorting method from nephritic and young MRL/lpr as well as NZB/W F1 mice and CD4-depleted, CD8-depleted or CD4- and CD8-depleted populations from lymph nodes were subjected to RT-PCR–SSCP. (a) Comparison of T cell clonality in different tissues between nephritic and young MRL/lpr mice. (b) Comparison of T cell clonality in different tissues between nephritic and young NZB/W F1 mice. Black triangles indicate the identical TCR Vβ clonotypes expanded in different organs. Lanes representative of different organs are indicated as arrows. Three individual mice were analysed in each group, and all mice yielded essentially the same results within each group.

Vβ6   N-Dβ-N   Jβ

kidney brain

(NZB x NZW)F1 (40 weeks)

C	A	S	S		I	·G	D		N	N	Q	A	
TGT	GCC	AGC	AGT		ATA	GGG	GAT		AAC	AAC	CAG	GCT	(Jβ1·5)

kidney brain

(NZB x NZW)F1 (47 weeks)

C	A	S	S		I	P	D	R		A	E	T	L	
TGT	GCC	AGC	AGT		ATC	CCG	GAC	AGG		GCA	GAA	ACG	CTG	(Jβ2·3)

kidney

MRL/lpr (22 weeks)

C	A	S	S		I	E	G		Y	E	Q	Y	
TGT	GCC	AGC	AGT		ATA	GAG	GGA		TAT	GAA	CAG	TAC	(Jβ2·6)

kidney

C	A	S	S		I	W	D	W	G	R		E	Q	Y	F	
TGT	GCC	AGC	AGT		ATT	TGG	GAC	TGG	GGG	AGG		GAA	CAG	TAC	TTC	(Jβ2·6)

MRL/lpr (26 weeks)

Fig. 2. The CDR3 sequence analysis of the TCR Vβ6 chain expressed by the identical clonotype accumulated in different organs from nephritic mice. Nucleotides and corresponding deduced amino acid sequences of the V(D)J junctional region of the identical TCR Vβ6 clones accumulated in the kidney and brain of nephritic NZB/W F1 and MRL/lpr mice are shown. Amino acid sequences are displayed in single letter code above the nucleotide sequences. Arrows indicate the identical bands at different sites that were sequenced. The indicated bands with the same migration from the left kidney and brain exhibited entirely identical CDR3 sequences. The common amino acid motif of 'I', 'D' or 'E' and 'G' found in these identical clonotypes from different individuals of the two strains were boxed, enlarged and underlined or simply underlined, respectively.

Table 1. The phenotype of T cells derived from nephritic NZB/W F1 mice

	Spleen		Kidney		Lung		Small intestine	
	CD69$^+$	CD62L^{low}	CD69$^+$	CD62L^{low}	CD69$^+$	CD62L^{low}	CD69$^+$	CD62L^{low}
Whole organ cells	6·35	18·87	3·11	6·92	4·82	15·77	1·69	6·37
CD4$^+$	16·68	48·55	23·19	58·94	21·37	73·25	23·34	89·09

Numbers shown are percentages of CD69$^+$ or CD62L^{low} cells either in the whole organ cell population or in the CD4$^+$ population. Experiments were conducted at least three times using different mice, and the data were not significantly different. Representative data are shown.

a massive increase in aberrant double-negative (CD4$^-$CD8$^-$) T cells (DN T cells), MRL/lpr mice demonstrated expansions in the CD4$^+$ population as well [2]. Although the lymphadenopathy in MRL/lpr mice is due primarily to the DN T cell accumulation, autoimmunities such as autoantibodies, vasculitis, arthritis and Ig-induced nephritis in this strain depend largely on CD4$^+$ T cells [3,4]. Similar results were also obtained from SLE patients in that the expanded CD4$^+$ T cell clonotypes were not restricted to the kidney but were also found in the peripheral blood and other

lesions, such as pleural and pericardial effusions of patients with lupus serositis, and these expansions correlated with the disease activities [16–18]. Our findings are consistent with the above studies, and to our knowledge this is the first report of the existence of identical CD4$^+$ T cell clonotypes having expanded in many organs of lupus mice. Because the CD4$^+$ T cell is important in the pathogenesis of lupus [3–7], our results suggest that the clonally expanded CD4$^+$ T cells in MRL/lpr and NZB/W F1 mice play an important role in the development of SLE. Our observation of
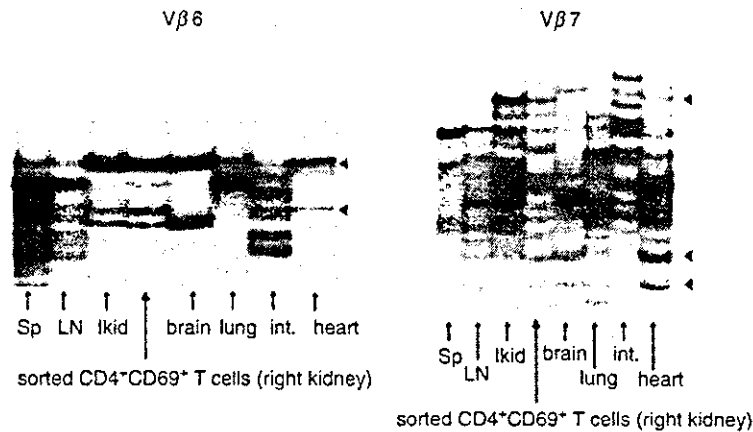
Vβ6   Vβ7

Sp LN lkid │ brain lung int. heart

sorted CD4⁻CD69⁺ T cells (right kidney)

Sp │ lkid │brain│ int. │
LN   │   lung heart

sorted CD4⁺CD69⁺ T cells (right kidney)

Fig. 3. Analysis of T cell clonality of FACS-sorted CD4⁻CD69⁺ from the right kidney of a NZB/W F1 nephritic mice at 47 weeks by RT-PCR-SSCP. FACS-sorted CD4⁺CD69⁺ cells from the right kidney and the whole T cell populations of other organs were subjected to RT-PCR-SSCP analysis to compare the expanded clonotypes of the sorted CD4⁻CD69⁺ population with those of the whole T cell populations in other organs, including the left kidney. Black triangles indicate identical expanded bands shared by the CD4⁺CD69⁺ population and the whole T cell populations in other organs. Lanes representative of different organs or sorted cells are indicated by arrows.

restricted Vβ usage in commonly expanded clones suggests that these CD4⁺ T cells were likely to be activated by a particular autoantigen(s). The restricted use of TCR Vβ genes in aged diseased mice has been reported in MRL/lpr [19,20] and NZB/W F1 [21,22] mice.

We further addressed whether these identical expanded CD4⁺ T cell clones are activated by specific antigen(s) by performing CDR3 sequence analysis of the TCR Vβ6 chain expressed on these T cell subsets in nephritic MRL/lpr and NZB/W F1 mice. We found that these TCR Vβ6 chains displayed a common amino acid residue motif of IXD or E and G in the CDR3 loops either in the brain or kidney in these two strains. These N(D)N regions encoding isoleucine gave rise to the sequence CASSI in TCR Vβ6 gene. These findings suggest that CD4⁺ T cells in these strains may recognize restricted epitopes on autoantigens, thus leading to the specific antigen-driven activation and resulting in clonal expansion and accumulation in different sites of diseased mice. Previous studies showed that CDR3 of the TCR Vβ chain expressed by pathogenic T cell clones in lupus mice bears a recurrent motif of anionic residues such as D or E. suggesting that it is specific for autoantigens with cationic residue [23–27]. Among several autoantigens predicted to be possibly involved in SLE to date, nucleosomes that carry cationic residues are believed to be primary immunogens that initiate the cognate interaction between the pathogenic T and B cells of SLE and induce the pathogenic anti-DNA autoantibodies [26,27]. The existence of a D motif in the CDR3 region found in our experiments is in accordance with those studies. Previous reports suggest the association of Vβ6 with autoreactivity by the increased expression of Vβ6 in MRL/lpr mice compared to control mice [28], and by the existence of autoreactive T cell lines with Vβ6 from lupus-prone SNF1 mice [29]. Although these reports may be consistent with our results, the actual evaluation of autoreactivity of expanded T cells should be clarified by the cloning of TCR of these T cells.

SSCP-bands could result from co-migration of the cDNA molecules with different sequences. Although definitive proof of clonal T cells requires further actual cloning and sequencing, we found co-migration to be a relatively rare phenomenon in SSCP

analysis, and each band we analysed was clearly derived from a single sequence (Fig. 2).

Our FACS analysis showed that the activated CD4⁺ T cells such as the CD4⁺CD69⁺ or CD4⁺CD62Lˡᵒʷ cell population were detected in the spleen, kidney, lung and small intestine in nephritic NZB/W F1 mice. This indicates that CD4⁺ T cells infiltrating into different sites of diseased lupus mice were activated. It has been demonstrated that the CD4⁺CD69⁺ population shared the same clonotypes as those commonly expanded clonotypes of whole T cell populations in other organs, including the left kidney. This observation revealed that the commonly expanded and accumulated T cell clonotypes in various organs in this lupus model contained CD4⁺ T cell of activated phenotype. Therefore, we concluded that some CD4⁺ T cells in nephritic lupus mice were activated, and it is the CD4⁻CD69⁺ phenotype that clonally expanded and accumulated in various sites. Thus these cells might be involved in the disease pathogenesis.

CD69 is known to be an early T cell activation marker that is involved in signal transduction, cell proliferation and cytokine secretion [30]. Previous reports have shown that the CD4⁺CD69⁺ subset of peripheral blood T cells was larger in SLE patients than in normal controls [31] and the percentage of CD4⁺CD69⁺ T cells correlated with the disease activity in SLE patients [32]. The expression of this subset was also found to be significantly increased in peripheral lymphoid tissues and inflammatory infiltrates in the kidney and lung of aged NZB/W F1 mice without skewing to a particular TCR Vβ usage [33]. Our results showed agreement with the above studies, suggesting that the clonally expanded CD4⁺CD69⁺ phenotypes in various organs may play an important role in SLE pathogenesis via signal transduction, cell proliferation and cytokine secretion.

As is well known, MRL/lpr mice which develop severe, progressive, systemic autoimmune disease spontaneously often exhibit a high incidence of inflammatory central nervous system (CNS) disease [34–36]. Previous studies showed the dominant infiltration of CD4⁺ T cells in brains from this strain [35], and anti-CD4 therapy effectively prevented the development of CNS lesions [37]. Our SSCP study revealed that the systemically

expanding CD4⁺ T cell clone also existed in the CNS of aged MRL/lpr mice. These results suggest that CD4⁺ T cells activated by systemic autoantigen migrate to the brain across the blood–brain barrier. The hypothesis in some degree may elucidate why the onset of CNS lesions in human SLE are often associated with disease severity and disease duration.

In summary, combining RT-PCR–SSCP analysis with the CDR3 sequence analysis of the TCR Vβ chain family expressed by T cell clones has allowed us to demonstrate that some CD4⁺ T cells are activated, clonally expanded and commonly accumulated in different tissues in nephritic MRL/lpr and NZB/W F1 lupus mice. These CD4⁺ T cell clonotypes might recognize restricted T cell epitopes on autoantigens and are involved in specific immune responses of SLE, thus playing a pathogenic role in these lupus mice.

ACKNOWLEDGEMENTS

REFERENCES

1 Rozzo SJ, Drake CG, Chiang BL *et al.* Evidence for polyclonal T cell activation in murine models of systemic lupus erythematosus. J Immunol 1994; 153:1340–51.

2 Giese T, Davidson WF. Evidence for early onset, polyclonal activation of T cell subsets in mice homozygous for lpr. J Immunol 1992; 149:3097–106.

3 Koh DR, Ho A, Rahemtulla A *et al.* Murine lupus in MRL/lpr mice lacking CD4 or CD8 T cells. Eur J Immunol 1995; 25:2558–62.

4 Jevnikar AM, Grusby MJ, Glimcher LH. Prevention of nephritis in major histocompatibility complex class II-deficient MRL-lpr mice. J Exp Med 1994; 179:1137–43.

5 Jabs DA, Burek CL, Hu Q *et al.* Anti-CD4 monoclonal antibody therapy suppresses autoimmune disease in MRL/Mp-lpr/lpr mice. Cell Immunol 1992; 141:496–507.

6 Santoro TJ, Portanova JP, Kotzin BL. The contribution of L3T4⁺ T cells to lymphoproliferation and autoantibody production in MRL-lpr/lpr mice. J Exp Med 1988; 167:1713–8.

7 Wofsy D, Seaman WE. Successful treatment of autoimmunity in NZB/NZW F1 mice with monoclonal antibody to L3T4. J Exp Med 1985; 161:378–91.

8 Sekigawa I, Okada T, Noguchi K *et al.* Class-specific regulation of anti-DNA antibody synthesis and the age-associated changes in (NZB × NZW) F1 hybrid mice. J Immunol 1987; 138:2890–5.

9 Chesnutt MS, Finck BK, Killeen N *et al.* Enhanced lymphoproliferation and diminished autoimmunity in CD4-deficient MRL/lpr mice. Clin Immunol Immunopathol 1998; 87:23–32.

10 Yamamoto K, Masuko K, Takahashi S *et al.* Accumulation of distinct T cell clonotypes in human solid tumors. J Immunol 1995; 154:1804–9.

11 Yamamoto K, Masuko-Hongo K, Tanaka A *et al.* Establishment and application of a novel T cell clonality analysis using single-strand conformation polymorphism of T cell receptor messenger signals. Hum Immunol 1996; 48:23–31.

12 Mixter PF, Russell JQ, Morrissette GJ *et al.* A model for the origin of TCR-alphabeta⁺ CD4⁻CD8⁻ B220⁺ cells based on high affinity TCR signals. J Immunol 1999; 162:5747–56.

13 Yamamoto K, Sakoda H, Nakajima T *et al.* Accumulation of multiple T cell clonotypes in the synovial lesions of patients with rheumatoid arthritis revealed by a novel clonality analysis. Int Immunol 1992; 4:1219–23.

14 Ikeda Y, Masuko K, Nakai Y *et al.* High frequencies of identical T cell clonotypes in synovial tissues of rheumatoid arthritis patients suggest the occurrence of common antigen-driven immune responses. Arthritis Rheum 1996; 39:446–53.

15 Komagata Y, Masuko K, Tashiro F *et al.* Clonal prevalence of T cells infiltrating into the pancreas of prediabetic non-obese diabetic mice. Int Immunol 1996; 8:807–14.

16 Mato T, Masuko K, Misaki Y *et al.* Correlation of clonal T cell expansion with disease activity in systemic lupus erythematosus. Int Immunol 1997; 9:547–54.

17 Kolowos W, Gaipl US, Voll RE *et al.* CD4 positive peripheral T cells from patients with systemic lupus erythematosus (SLE) are clonally expanded. Lupus 2001; 10:321–31.

18 Kato T, Kurokawa M, Sasakawa H *et al.* Analysis of accumulated T cell clonotypes in patients with systemic lupus erythematosus. Arthritis Rheum 2000; 43:2712–21.

19 Singer PA, Theofilopoulos AN. T-cell receptor V beta repertoire expression in murine models of SLE. Immunol Rev 1990; 118:103–27.

20 Singer PA, McEvilly RJ, Noonan DJ *et al.* Clonal diversity and T-cell receptor beta-chain variable gene expression in enlarged lymph nodes of MRL-lpr/lpr lupus mice. Proc Natl Acad Sci USA 1986; 83:7018–22.

21 Hirose S, Tokushige K, Kinoshita K *et al.* Contribution of the gene linked to the T cell receptor beta chain gene complex of NZW mice to the autoimmunity of (NZB × NZW) F1 mice. Eur J Immunol 1991; 21:823–6.

22 Yanagi Y, Hirose S, Nagasawa R *et al.* Does the deletion within T cell receptor beta-chain gene of NZW mice contribute to autoimmunity in (NZB × NZW) F1 mice? Eur J Immunol 1986; 16:1179–82.

23 Datta SK, Patel H, Berry D. Induction of a cationic shift in IgG anti-DNA autoantibodies. Role of T helper cells with classical and novel phenotypes in three murine models of lupus nephritis. J Exp Med 1987; 165:1252–68.

24 Suzuki N, Harada T, Mizushima Y *et al.* Possible pathogenic role of cationic anti-DNA autoantibodies in the development of nephritis in patients with systemic lupus erythematosus. J Immunol 1993; 151:1128–36.

25 Desai-Mehta A, Mao C, Rajagopalan S *et al.* Structure and specificity of T cell receptors expressed by potentially pathogenic anti-DNA autoantibody-inducing T cells in human lupus. J Clin Invest 1995; 95:531–41.

26 Mohan C, Adams S, Stanik V *et al.* Nucleosome: a major immunogen for pathogenic autoantibody-inducing T cells of lupus. J Exp Med 1993; 177:1367–81.

27 Adams S, Leblanc P, Datta SK. Junctional region sequences of T-cell receptor beta-chain genes expressed by pathogenic anti-DNA autoantibody-inducing helper T cells from lupus mice: possible selection by cationic autoantigens. Proc Natl Acad Sci USA 1991; 88:11271–5.

28 Mountz JD, Smith TM, Toth KS. Altered expression of self-reactive T cell receptor V beta regions in autoimmune mice. J Immunol 1990; 144:2159–66.

29 Adams S, Zordan T, Sainis K, Datta S. T cell receptor V beta genes expressed by IgG anti-DNA autoantibody-inducing T cells in lupus nephritis: forbidden receptors and double-negative T cells. Eur J Immunol 1990; 20:1435–43.

30 Cebrian M, Yague E, Rincon M *et al.* Triggering of T cell proliferation through AIM, an activation inducer molecule expressed on activated human lymphocytes. J Exp Med 1988; 168:1621–37.

31 Crispin JC, Martinez A, de Pablo P *et al.* Participation of the CD69 antigen in the T-cell activation process of patients with systemic lupus erythematosus. Scand J Immunol 1998; 48:196–200.

32 Portales-Perez D, Gonzalez-Amaro R, Abud-Mendoza C *et al.* Abnormalities in CD69 expression, cytosolic pH and Ca²⁺ during activation of lymphocytes from patients with systemic lupus erythematosus. Lupus 1997; 6:48–56.

33 Ishikawa S, Akakura S, Abe M *et al.* A subset of CD4⁺ T cells expressing early activation antigen CD69 in murine lupus: possible abnormal regulatory role for cytokine imbalance. J Immunol 1998; 161:1267–73.

34 Alexander EL, Murphy ED, Roths JB *et al.* Congenic autoimmune murine models of central nervous system disease in connective tissue disorders. Ann Neurol 1983; 14:242–8.

35 Vogelweid CM, Johnson GC, Besch-Williford CL *et al.* Inflammatory central nervous system disease in lupus-prone MRL/lpr mice: comparative histologic and immunohistochemical findings. J Neuroimmunol 1991; 35:89–99.

36 Hess DC, Taormina M, Thompson J *et al.* Cognitive and neurologic deficits in the MRL/lpr mouse: a clinicopathologic study. J Rheumatol 1993; 20:610–7.

37 O'Sullivan FX, Vogelweid CM, Besch-Williford CL *et al.* Differential effects of CD4+ T cell depletion on inflammatory central nervous system disease, arthritis and sialadenitis in MRL/lpr mice. J Autoimmun 1995; 8:163–75.

Potentiation of Tumor Eradication by Adoptive Immunotherapy with T-cell Receptor Gene-Transduced T-Helper Type 1 Cells

Kenji Chamoto,[1] Takemasa Tsuji,[1] Hiromi Funamoto,[1] Akemi Kosaka,[1] Junko Matsuzaki,[1] Takeshi Sato,[1] Hiroyuki Abe,[1] Keishi Fujio,[2] Kazuhiko Yamamoto,[2] Toshio Kitamura,[3] Tsuguhide Takeshima,[1] Yuji Togashi,[1] and Takashi Nishimura[1]

[1]Division of Immunoregulation, Section of Disease Control, Institute for Genetic Medicine, Hokkaido University, Sapporo, Japan, and [2]Department of Allergy and Rheumatology, Graduate School of Medicine, and [3]Division of Cellular Therapy, Institute of Medical Science, University of Tokyo, Tokyo, Japan

ABSTRACT

Adoptive immunotherapy using antigen-specific T-helper type 1 (Th1) cells has been considered as a potential strategy for tumor immunotherapy. However, its application to tumor immunotherapy has been hampered by difficulties in expanding tumor-specific Th1 cells from tumor-bearing hosts. Here, we have developed an efficient protocol for preparing mouse antigen-specific Th1 cells from nonspecifically activated Th cells after retroviral transfer of T-cell receptor (TCR)-α and TCR-β genes. We demonstrate that Th1 cells transduced with the TCR-α and -β genes from the I-A^d-restricted ovalbumin (OVA)$_{323-339}$-specific T-cell clone DO11.10 produce IFN-γ but not interleukin-4 in response to stimulation with OVA$_{323-339}$ peptides or A20 B lymphoma (A20-OVA) cells expressing OVA as a model tumor antigen. TCR-transduced Th1 cells also exhibited cytotoxicity against tumor cells in an antigen-specific manner. Moreover, adoptive transfer of TCR-transduced Th1 cells, but not mock-transduced Th1 cells, exhibited potent antitumor activity in vivo and, when combined with cyclophosphamide treatment, completely eradicated established tumor masses. Thus, TCR-transduced Th1 cells are a promising alternative for the development of effective adoptive immunotherapies.

INTRODUCTION

T-helper type 1 (Th1)-dominant immunity, which is regulated by interleukin (IL)-12 and IFN-γ, plays a crucial role for the eradication of tumors in vivo (1, 2). However, the production of Th1 cytokines such as IL-2 and IFN-γ is markedly suppressed in the majority of tumor-bearing hosts (3, 4). Such defects in Th1-mediated immunity in tumor-bearing hosts have made it difficult to induce tumor-specific CTLs that promote tumor rejection (5). Therefore, it is critically important to develop methods that promote Th1-dominant immunity at the local tumor site.

In a previous study (6), we demonstrated that adoptively transferred Th1 cells exhibit strong antitumor activity in vivo and can eradicate an established tumor mass. Moreover, in contrast to Th2 cells, Th1-cell therapy is beneficial for inducing immunological memory in tumor-specific CTLs (6). These findings indicate that Th1-cell therapy is an effective strategy to introduce local T-cell help that overcomes strong immunosuppression in tumor-bearing hosts. However, the application of Th1 cells to adoptive tumor immunotherapy has been hampered by difficulties in inducing sufficient numbers of tumor antigen-specific Th1 cells.

Recently, it has become possible to introduce T-cell receptor (TCR)-α and -β genes into T cells by retroviral transduction (7-10). We used this technology to introduce TCR transgenes specific for the model tumor antigen ovalbumin (OVA) into anti-CD3-activated Th1-

polarized CD4$^+$ T cells. We show that TCR-transduced Th1 cells produce IFN-γ but not IL-4 in response to OVA$_{323-339}$ peptides. Moreover, we show that adoptively transferred TCR-transduced Th1 cells, when combined with cyclophosphamide (CY) treatment, can completely eradicate A20-OVA tumor masses. These findings indicate that TCR transduction of nonspecific Th1 cells is an effective strategy for introducing local T-cell help in the tumor-bearing host.

MATERIALS AND METHODS

Mice. BALB/c mice were obtained from Charles River Japan (Yokohama, Japan). OVA$_{323-339}$-specific I-A^d-restricted TCR-transgenic mice (DO11.10) maintained on the BALB/c background were kindly donated by Dr. K. M. Murphy (Washington University School of Medicine, St. Louis, MO; Ref. 6). All of the mice were female and were used at 5-6 weeks of age.

Cytokines, mAbs, and Antigen. IL-12 was kindly donated by Genetics Institute (Cambridge, MA). IL-2 was supplied by Takuko Sawada (Shionogi Pharmaceutical Institute Co. Ltd., Osaka, Japan). Anti-IL-4 monoclonal antibody (mAb; 11B11) was purchased from American Type Culture Collection (Manassas, VA). PE-anti-CD4 mAb, FITC-anti-CD45RB mAb, FITC-anti-CD8 mAb, purified anti-CD3 mAb, PerCP-anti-CD3 mAb, FITC-anti-IFN-γ mAb, and anti-IFN-γ mAb (R4-6A2) were purchased from PharMingen (San Diego, CA). KJ1-26 mAb was kindly donated by Dr. K. M. Murphy (Washington University School of Medicine, St. Louis, MO). Recombinant IFN-γ was purchased from Pepro Tech EC Ltd. (London, England). OVA$_{323-339}$ peptide was kindly supplied by Dr. H. Tashiro (Fujiya Co. Ltd., Hadano, Japan).

Generation of OVA-Specific Th1 Cells from DO11.10 Mice. CD4$^+$ CD45RB$^+$ naive T cells were isolated from nylon-passed spleen cells from DO11.10 TCR-transgenic mice using FACSVantage (Becton Dickinson. San Jose, CA) as reported previously (6). Purified CD4$^+$ CD45RB$^+$ cells were stimulated with 10 μg/ml OVA$_{323-339}$ peptide in the presence of mitomycin C-treated BALB/c spleen cells, 20 units/ml IL-12, 1 ng/ml IFN-γ, 50 μg/ml anti-IL-4 mAb, and 20 units/ml IL-2 for Th1 development. At 48 h, cells were restimulated with OVA$_{323-339}$ under the same conditions and were used at 9-12 days of culture.

Construction of Retrovirus Vectors. Complementary DNAs encoding MHC class II-restricted OVA-specific TCR-α and -β genes were amplified from cDNA of CD4$^+$ T cells of DO11.10 mice by reverse transcription-PCR as described previously (7). TCR-α and -β cDNAs were inserted into EcoRI and NotI sites within the multiple cloning site of the pMX vector, and were designated as pMX-DOTAE and pMX-DOTBE, respectively (7).

Preparation of Retroviruses and Infection of Nonspecific Th1 Cells. Recombinant retroviruses were produced as described previously (7). Briefly, pMX-DOTAE or pMX-DOTBE vector, which were kindly donated by Dr. T. Kitamura (Institute of Medical Science, University of Tokyo, Tokyo, Japan), were transfected into PLAT-E by using FuGENE 6 transfection reagent (Roche, Indianapolis, IN). Twenty-four h later, supernatants were replaced with fresh medium. After incubation for an additional 24 h, supernatants containing the retroviruses were harvested and stored at −80°C until use. Nonspecific Th1 cells were induced from isolated CD4$^+$CD45RB$^+$ naive T cells of BALB/c mice by stimulation with 2 μg/ml anti-CD3 mAb in the presence of mitomycin C-treated BALB/c spleen cells in Th1 cytokine conditions, as described above. Twenty-four h after stimulation, these CD4$^+$ T cells were coinfected by retroviruses carrying pMX-DOTAE and pMX-DOTBE in 12-well plates coated with retronectin and anti-CD3 mAb. This

386

infection procedure was carried out three times at 8-h intervals. At 4 days, the expression of DO11.10 TCR was examined by FITC-conjugated KJ1–26 mAb, which is a clonotypic mAb to DO11.10 TCR. These KJ1–26⁺ cells were isolated with MACS beads (Miltenyi Biotec Inc., Auburn, CA) at over 98% purity and were expanded under Th1 conditions until day 6. More than 90% of Th cells, expanded in this Th1 condition, showed IFN-γ-producing ability but no IL-4-producing ability. As a control, polyclonally activated Th1 cells were transduced with pMX-internal ribosomal entry site (IRES) green fluorescent protein (GFP) vector and used as Mock-GFP gene-transduced Th1 cells.

Flow Cytometry. The phenotypic characterization of Th1 cells was carried out using a FACSCalibur flow cytometer (Becton Dickinson, San Jose, CA) and Cell Quest software. Fluorescence data were collected with logarithmic amplification. For each sample, data from 10,000 volume-gated viable cells were collected. Mean fluorescence intensity was calculated using the Cell Quest program.

Intracellular Cytokine Expression. For the detection of cytoplasmic cytokine expression, cells stimulated with immobilized anti-CD3 mAb for 6 h in the presence of brefeldin A were first stained with FITC-conjugated anti-KJ1–26 mAb and PerCP-anti-CD4 mAb, fixed with 4% paraformaldehyde, treated with permeabilizing solution [50 mM NaCl, 5 mM EDTA, 0.02% NaN₃, and 0.5% Triton X-100 (pH 7.5)], and these cells were then stained with PE-conjugated anti-IL-4 mAb or anti-IFN-γ mAb for 45 min on ice. The percentage of cells expressing cytoplasmic IL-4 or IFN-γ was determined by flow cytometry (FACSCalibur; Becton Dickinson, San Jose, CA).

Cytokine Levels. The levels of IFN-γ or IL-4 in culture supernatants were measured by OptEIA mouse IFN-γ and OptEIA mouse IL-4 (PharMingen), respectively.

Cytotoxicity Assay. The cytotoxicity mediated by Th1 cells was measured by 4-h ⁵¹Cr-release assays as described previously (11). Tumor-specific cytotoxicity was determined using A20-OVA (H-2ᵈ) as target cells. As a control, parental A20 cells (H-2ᵈ) were used. The percentage of cytotoxicity was calculated as described previously (11).

Tumor Cell Therapy Using Th1 Cells Combined with CY. A20-OVA cells (2 × 10⁶) were inoculated intradermally into BALB/c mice. When the tumor mass became palpable (6–8 mm), the tumor-bearing mice were treated with none, CY, CY + TCR-transduced Th1 cells, CY + mock-transduced Th1 cells. TCR-transduced Th1 cells, or mock-transduced Th1 cells. Th1 cells (5 × 10⁶ cells/mouse) were i.v. transferred into tumor-bearing mice 1 day after i.p. injection of CY (80 mg/kg). The antitumor activity mediated by the transferred cells was determined by measuring tumor size in perpendicular diameters. Tumor volume was calculated by the following formula: tumor volume = 0.4 × length (mm) × [width (mm)]² (12). Tumor-bearing mice that survived for more than 60 days after therapy were considered completely cured. The mean of five mice per group is indicated in graphs.

RESULTS AND DISCUSSION

We have previously developed an adoptive tumor immunotherapy protocol, using Th1-polarized TCR transgenic T cells specific for the model tumor antigen ovalbumin (OVA) presented by I-Aᵈ. To evaluate the utility of retroviral gene transduction as a tool for generating tumor antigen-specific Th1 cells, we introduced the TCR-α and -β chain genes from the DO11.10 T-cell clone into polyclonally activated T cells by retroviral vectors. Specifically, we isolated CD4⁺CD45RB⁺ naive CD4⁺ T cells from wild-type BALB/c mouse spleen cells and activated these cells with anti-CD3 mAb under Th1-inducing conditions (IL-12 + IFN-γ + anti-IL-4 mAb) in the presence of mitomycin C-treated spleen cells as antigen presenting cells, which is essential for the cross-linking of soluble anti-CD3 mAbs. After 24 h of culture, the cells were retrovirally transduced with DO11.10 TCR-α and -β genes or a mock-GFP gene (three successive gene transductons 8 h apart). TCR- or mock-transduced Th cells were cultured for another 3 days in Th1-inducing conditions. Then, the expression of DO11.10 TCR on expanded cells was examined by flow cytometry. TCR expression was evaluated with the clonotypic KJ1–26 mAb, which stains most CD4⁺ T cells in DO11.10 transgenic mice (Fig. 1B), but very few T cells from normal mice (Fig.
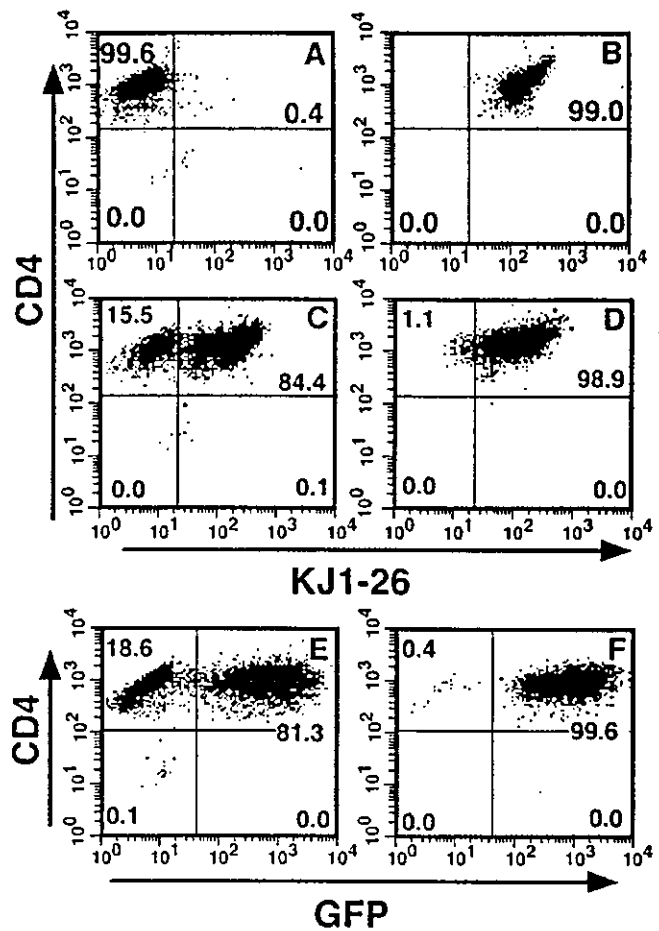

KJ1-26

GFP

Fig. 1. Retroviral transfer of DO11.10 T-cell receptor (TCR)-α and -β chain genes into anti-CD3 monoclonal antibody (mAb)-activated nonspecific T-cell helper (Th) cells. Naïve Th cells prepared from BALB/c mice were activated with anti-CD3 mAb for 24 h, and these cells were then retrovirally transduced with DO11.10 TCR genes (C, D) or with a mock gene containing green fluorescent protein (GFP: E, F), and expanded under Th type 1 (Th1)-inducing conditions, as described in "Materials and Methods." Four days after initiation of the culture, expression of the DO11.10 TCR recognized by KJ1–26 clonotypic mAb (C) or of the mock gene labeled with GFP (E) was determined by flow cytometry. Then, gene-transduced KJ1–26⁺ Th (D) or GFP⁺ Th cells (F) were isolated by MACS. As negative and positive controls for DO11.10 TCR expression, anti-CD3 mAb-activated Th cells derived from wild-type BALB/c mice (A), and Th1 cells derived from DO11.10 TCR transgenic mice (B) were used, respectively. Similar data were obtained in three independent experiments.

1A). The majority (84%) of anti-CD3-activated CD4⁺ T cells successfully expressed DO11.10 TCR detected by KJ1–26 mAb (Fig. 1C) or a mock gene detected by GFP expression (Fig. 1E) after retroviral transduction.

To investigate the function of DO11.10 TCR-transduced Th cells, KJ1–26-expressing cells were enriched by MACS beads (Fig. 1D). As a control, GFP-expressing Th cells were isolated by fluorescence-activated cell sorting (Fig. 1F). As shown in Fig. 1, D and F, we could prepare retrovirally modified Th cells expressing DO11.10 TCR and mock-GFP Th cells that were >98% pure. We examined the cytokine producing ability of DO11.10 TCR gene-transduced Th cells by intracellular staining after stimulation with the cognate I-Aᵈ-binding OVA₃₂₃₋₃₃₉ peptide. As shown in Fig. 2, B and F, DO11.10 TCR-transduced Th cells detected by KJ1–26 mAb produced IFN-γ but not IL-4 in response to OVA-peptide. In sharp contrast, mock-GFP-transduced Th1 cells produced neither IFN-γ nor IL-4 in response to stimulation with OVA₃₂₃₋₃₃₉ (Fig. 2, D and H). We further demonstrated that DO11.10 TCR-transduced Th1 cells exhibit high levels of

387

Fig. 2. DO11.10 T-cell receptor (TCR)-transduced T-helper type 1 (Th1) cells produce IFN-γ but not interleukin (IL)-4 in response to stimulation with the I-A^d-restricted ovalbumin (OVA)$_{323-339}$ peptide. Th cells were transduced with DO11.10 TCR genes or with a mock green fluorescent protein (GFP) gene and induced into Th1 cells, as described in "Materials and Methods." After culture for 7 days, KJ1-26$^+$ TCR-transduced Th1 cells (A, B, E, and F) and GFP$^+$ mock gene-transduced Th1 cells (C, D, G, and F) were stimulated with (B, D, F, and H) or without (A, C, E, and G) OVA$_{323-339}$ peptide. After 24 h of culture, cytokine-producing ability of cells was determined by intracellular staining: IFN-γ producing ability of TCR-transduced Th1 cells (A, B) or mock gene-transduced Th1 cells (C, D); IL-4 producing ability of TCR-transduced Th1 cells (E, F) or mock gene-transduced Th1 cells (G, H). The figures in data represent the percentage of cytokine-producing cells. Similar results were obtained in three separate experiments.
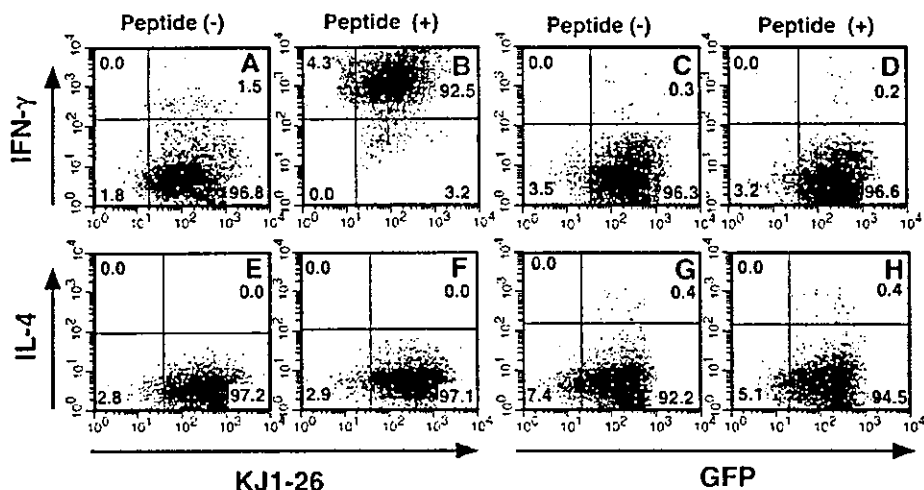
IFN-γ but not IL-4 production in response to stimulation with OVA-peptide-pulsed A20 tumor cells (Fig. 3, A and B). In addition to cytokine production, TCR-transduced Th1 cells, but not mock-transduced Th1 cells, exhibited strong cytotoxicity against antigenic peptide-pulsed A20 cells (Fig. 3C). When compared with Th1-polarized DO11.10 cells (DO11.10-Th1) from transgenic animals, the response of TCR-transduced Th1 cells to the cognate OVA peptide was lower than DO11.10-Th1 cells, although they exhibited a very similar response at a higher dose (2 μg/ml) of peptide (Fig. 3D). Such different responsiveness was also demonstrated when we used A20-OVA tumor stimulator, which exhibited lower stimulation activity compared with peptide-pulsed A20 tumor cells. As shown in Fig. 3, E and F, TCR-transduced Th1 cells showed lower IFN-γ production and cytotoxicity in response to A20-OVA tumor compared with DO11.10-Th1 cells. As shown in Fig. 1D, the expression intensity of genetically modified TCR is always lower than that of physiologically expressing

Fig. 3. T-cell receptor (TCR)-transduced T-helper type 1 (Th1) cells demonstrate both IFN-γ production and cytotoxicity in response to ovalbumin (OVA)$_{323-339}$ peptide-pulsed A20 tumor cells and A20-OVA tumor cells. Th1 cells transduced with DO11.10 TCR genes were induced as described in "Materials and Methods." After culture for 7 days, KJ1-26$^+$ TCR-transduced Th1 cells (TCR-Th1) were harvested and cultured with (■) or without (□) OVA$_{323-339}$ peptide [with, OVA-pep (+); without, OVA-pep (−)] in the presence of mitomycin C-treated spleen cells to determine their ability to produce IFN-γ (A) or interleukin (IL)-4 (B). As negative control cells, Th1 cells transduced with a mock green fluorescent protein (GFP) gene (A, B; GFP-Th1) were used. C, cytotoxic activity of TCR-Th1 (O, ●) and GFP-Th1 cells (△, ▲) against unpulsed A20 tumor cells (O, △) or OVA$_{323-339}$ peptide-pulsed A20 tumor cells (●, ▲) was measured by 4-h ^{51}Cr-release assay. D, TCR-Th1 or Th1 cells induced from DO11.10 transgenic mice (DO11.10-Th1) were stimulated with three different doses of peptide (0, □; 0.02,[gbox]; 0.2,[rhbox]; 2 μg/ml, ■). After 24 h, IFN-γ levels of culture supernatants were measured by ELISA. E, IFN-γ-producing ability of TCR-Th1 or DO11.10-Th1 by stimulation with A20-OVA (■) or A20 (□) tumor cells. F, cytotoxicity of TCR-Th1 (O, ●) or DO11.10-Th1 (△, ▲) against A20-OVA (●, ▲) or A20 (O, △) tumor cells was measured by 4-h ^{51}Cr-release assay. The bars, mean ± SE of triplicate samples. Similar results were obtained in three separate experiments.

DO11.10 TCR (Fig. 1B). Therefore, the lower responsiveness of TCR-transduced Th1 cells may be derived from lower expression intensity or affinity of genetically modified TCR compared with physiologically expressing TCR. In contrast to TCR-transduced Th1 cells, mock-transduced Th1 cells exhibited no significant IFN-γ production and cytotoxicity by stimulation with I-A^d-binding OVA-peptide (Fig. 3, A–C).

Finally, we investigated the therapeutic activity of TCR-transduced Th1 cells against tumor-bearing mice. BALB/c mice were inoculated with A20-OVA tumor cells and, when the tumor mass became palpable (6–8 mm), TCR-transduced Th1, mock-transduced Th1 cells, or DO11.10-derived Th1 cells were i.v. transferred. Consistent with previous results (6), transfer of 2 × 10^7 DO11.10-derived Th1 cells induced complete cure of all tumor-bearing mice. However, neither TCR-transduced Th1 cells nor mock-transduced Th1 cells exhibited significant antitumor activity in vivo, even when 2 × 10^7 cells were transferred (Fig. 4A). This lower antitumor activity of TCR-transduced Th1 cells might be due to lower intensity or affinity of genetically modified TCR as described above. Alternatively, down-modulation of retrovirally transduced TCR expression by transcriptional silencing mechanisms (13) might influence the antitumor activity of TCR-transduced Th1 cells in vivo. As shown in Fig. 4B, we found that the therapeutic efficacy of Th1 cells was augmented by combination therapy with CY. Namely, the transfer of 5 × 10^6 DO11.10-Th1 cells combined with CY pretreatment caused complete rejection of tumor, although Th1 cells alone exhibited no significant antitumor activity. Such potentiation by CY treatment was observed even when tumor-bearing mice were transferred with 2 × 10^6 Th1 cells.[4] Therefore, we examined whether therapeutic efficacy of TCR-transduced Th1 cells could be potentiated by combination with CY treatment. Neither TCR-transduced Th1 cells (5 × 10^6) nor mock-transduced Th1 cells showed significant antitumor activity in vivo. However, when tumor-bearing mice were pretreated with CY (80 mg/kg) 1 day before the transfer of TCR-transduced Th1 cells (5 × 10^6), tumor growth was strongly inhibited (Fig. 4C). All of the mice treated with CY plus TCR-transduced Th1 cells were completely cured from tumors (Fig. 4D). Such potentiation by CY was not observed when 2 × 10^6 TCR-transduced Th1 cells were transferred into tumor-bearing mice. Therefore, physiological DO11.10 TCR-expressing Th1 cells appeared to exhibit >2-fold stronger antitumor activity in vivo compared with TCR-transduced Th1 cells. Thus, combined therapy with
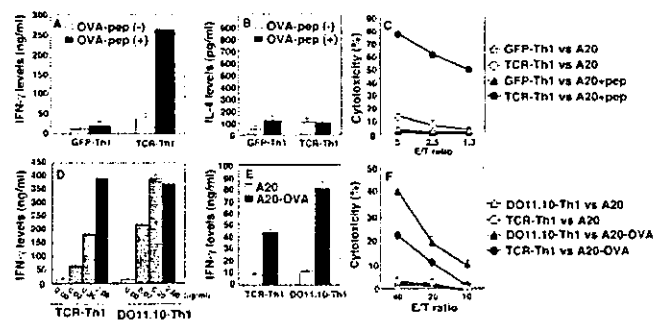
388